



AMERICAN UNIVERSITY OF BEIRUT

THERAPEUTIC OPPORTUNITIES IN TARGETING THE  
PENTOSE PHOSPHATE PATHWAY IN COLORECTAL  
CANCER

by  
NOORHAN AMER GHANEM

A thesis  
submitted in partial fulfillment of the requirements  
for the degree of Master of Science  
to the Department of Biochemistry and Molecular Genetics  
of the Faculty of Medicine  
at the American University of Beirut

Beirut, Lebanon  
June 2020

AMERICAN UNIVERSITY OF BEIRUT

THERAPEUTIC OPPORTUNITIES IN TARGETING THE  
PENTOSE PHOSPHATE PATHWAY IN COLORECTAL  
CANCER

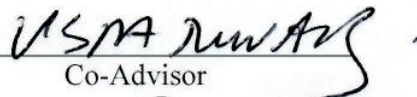
by  
NOORHAN AMER GHANEM

Approved by:


\_\_\_\_\_  
Dr. Nadine Darwiche, Professor  
Biochemistry and Molecular Genetics

  
Advisor

\_\_\_\_\_  
Dr. Julnar Usta, Professor  
Biochemistry and Molecular Genetics

  
Co-Advisor

\_\_\_\_\_  
Dr. Georges Nemer, Professor  
Biochemistry and Molecular Genetics

  
Member of Committee

\_\_\_\_\_  
Dr. Riyad El-Khoury, Assistant Professor  
Department of Pathology and Laboratory Medicine

  
Member of Committee

Date of thesis defense: June 19, 2020

# AMERICAN UNIVERSITY OF BEIRUT

## THESIS, DISSERTATION, PROJECT RELEASE FORM

Student Name:

Ghanem Noorhan Amer  
Last First Middle

Master's Thesis

Master's Project

Doctoral Dissertation

I authorize the American University of Beirut to: (a) reproduce hard or electronic copies of my thesis, dissertation, or project; (b) include such copies in the archives and digital repositories of the University; and (c) make freely available such copies to third parties for research or educational purposes.

I authorize the American University of Beirut, to: (a) reproduce hard or electronic copies of it; (b) include such copies in the archives and digital repositories of the University; and (c) make freely available such copies to third parties for research or educational purposes  
after: **One ---- year from the date of submission of my thesis, dissertation, or project.**  
**Two ---- years from the date of submission of my thesis, dissertation, or project.**  
**Three ---- years from the date of submission of my thesis, dissertation, or project.**

Noorhan Ghanem July 6, 2020

Signature

Date

## ACKNOWLEDGEMENTS

First and foremost, I would like to express my gratitude to Dr. Nadine Darwiche, my advisor, for supporting me and being a role model for me throughout this Master journey. I have certainly learned a lot from you, particularly on how to become a scientist in the biomedical research field. Thank you for advising me, guiding me, and for always reminding us how proud you were of us and of the importance of the work that we do.

I also want to extend my appreciation to Dr. Julnar Usta, my co-advisor, for being very caring. Thank you for your advise and guidance all along the way and for helping us decipher the many questions that arose during the course of this project, and for your expertise on cellular metabolism.

Thank you to Drs. Georges Nemer and Riyad El-Khoury for being part of my thesis committee, for reading my thesis, and for your useful thesis feedback.

I have to recognize Dr. Chirine El-Baba for being like a sister and continuously helping me out when I needed it. I will always remember our times together. Thank you, Chirine!

A huge thank you to all the Blue lab members, for being there and always having a solution when there just seemed to be none. The work being done in that lab is amazing, so continue on doing it!

Thank you to my dear friends whom I had at AUB. You made my Masters experience all the lot more memorable.

Thank you my very dear and loving parents, siblings, and family, for your continuous and endless support throughout all of this and for bearing with me even when I couldn't handel it all myself.

All praises be to Allah SWT for bestowing His grace and mercy upon us. TRULY, it is because of Him that this dream has become possible!

May this work contribute to the benefit of humanity...

# AN ABSTRACT OF THE THESIS OF

Noorhan Amer Ghanem

for

Master of Science

Major: Biochemistry

Title: Therapeutic Opportunities in Targeting the Pentose Phosphate Pathway in Colorectal Cancer

**Introduction:** Colorectal cancer (CRC) is the third most common neoplasia and the second cause of cancer-related deaths worldwide. Unlike normal cells, tumor cells deregulate their metabolism and rely on aerobic glycolysis (Warburg effect). CRC cells upregulate the pentose phosphate pathway (PPP), and p53 is a crucial regulator. The PPP is a significant route for glucose catabolism and is required for DNA synthesis of rapidly-proliferating cells. Its oxidative phase, catalyzed by the rate-limiting enzyme glucose-6-phosphate dehydrogenase (G6PD), provides the cell with nicotinamide adenine dinucleotide phosphate (NADPH) that has biosynthetic and detoxifying functions, particularly against the generation of reactive oxygen species (ROS). 5-Fluorouracil (5-FU) is the treatment of choice in CRC. However, 5-FU exhibits high toxicity and drug resistance. Therefore, we hypothesized that targeting the PPP might offer novel therapeutic opportunities in CRC and improve the response to 5-FU. We aimed to investigate and characterize the anti-tumor effect of G6PD inhibitors (6-aminonicotinamide (6-AN), dehydroepiandrosterone (DHEA), and polydatin) alone, or in combination with 5-FU on the PPP in CRC cells.

**Methods:** Assess the effect of G6PD inhibitors and 5-FU alone or in combination using cell viability assays (MTT, SRB) on CRC cell lines of different p53 and 5-FU resistance status. Synergistic effects are estimated using Compusyn software. Determine the mechanism of action of the combination treatment on cell cycle and cell death using propidium iodide, and immunoblotting assays. PPP-related enzymes' (G6PD, transketolase) product levels and/or activities are measured. ROS levels and glutathione peroxidase (GPx) activity are evaluated.

**Results:** *In silico* analysis revealed elevated G6PD mRNA in CRC versus normal tissue. The tested G6PD inhibitors reduced CRC cell viability. 6-AN synergized with 5-FU treatment in HCT116 cells. Furthermore, 6-AN sensitized HCT116-5-FU resistant and HCT116 p53<sup>-/-</sup> cells to 5-FU treatment. The 6-AN/5-FU combination treatment induced cell cycle arrest in different phases and accumulation of treated HCT116 and HCT116 p53<sup>-/-</sup> cells in the sub-G1 phase. The 6-AN/5-FU combination reduced the activity of G6PD compared to single treatments while G6PD and transketolase levels remain unaltered. ROS levels and GPx activity increased upon treatment. CRISPR/Cas9 G6PD knockout HCT116 cells are being developed.

**Conclusion:** These findings reveal that combining G6PD inhibitors with 5-FU decrease resistance and further sensitize CRC cells to 5-FU treatment independently of p53 and 5-FU drug resistance status. Exploiting the metabolic vulnerability of cancer offer a novel clinical approach in colorectal cancer management.

# CONTENTS

ACKNOWLEDGMENTS .....	V
ABSTRACT.....	VI
LIST OF ILLUSTRATIONS .....	X
LIST OF TABLES .....	XII
LIST OF ABBREVIATIONS .....	XIII

## Chapter

I- INTRODUCTION.....	1
A- Colorectal Cancer .....	1
a. Incidence and Statistics.....	1
b. Risk Factors, Symptoms, Diagnosis, and Prognosis.....	2
c. Development and Genetic Background of Colorectal Cancer	3
d. Treatment.....	4
1- 5-FU Resistance .....	5
B- Cancer Metabolism .....	6
a. Overview.....	6
b. Pentose Phosphate Pathway .....	9
1- Oxidative Phase .....	12
2- Non-Oxidative Phase .....	13
3- Regulation.....	13
c. Pentose Phosphate Pathway Deregulation in Cancer	

Metabolism .....	14
C- Pentose Phosphate Pathway Inhibitors .....	16
a. Polydatin .....	16
b. DHEA .....	18
c. 6-AN .....	19
d. Combination Therapies .....	21
II- RATIONALE, SPECIFIC AIMS, AND SIGNIFICANCE .....	23
III- MATERIAL AND METHODS .....	25
A- <i>In Silico</i> Analysis .....	25
B- Cell Culture .....	25
1- <i>In Vitro</i> Human Models of Colorectal Cancer .....	25
a- HCT116 .....	25
b- HCT116 5FU-R .....	26
c- HCT116 p53 <sup>-/-</sup> .....	26
2- Cell Culture Conditions .....	27
C- MTT Proliferation Assay .....	27
D- SRB Viability Assay .....	28
E- Compusyn Synergy Software .....	28
F- Nitroblue Tetrazolium Reduction Assay .....	29
G- Cell Cycle Analysis .....	29
H- G6PD Activity Assay .....	30
I- TKT Quantitative ELISA Assay .....	31
J- GPx Activity Assay .....	32
K- Western Blotting .....	33
L- Statistical Analysis .....	34



IV- RESULTS.....	35
A. <i>In Silico</i> Analysis .....	35
B. G6PD inhibitors suppress the growth of different colorectal cancer cells.....	36
1- Polydatin Treatment.....	36
2- DHEA Treatment.....	37
3- 6-AN Treatment.....	38
C. G6PD inhibitors in combination with 5-FU further suppress the growth of different colorectal cancer cells .....	42
1- Polydatin 5-FU Combination .....	42
2- DHEA 5-FU Combiation .....	44
3- 6-AN 5-FU MTT Combination.....	45
4- 6-AN 5-FU SRB Combination.....	47
D. 6-AN and/or 5-FU treatment did not modify G6PD nor TKT protein levels but reduced G6PD activity .....	48
E. 6-AN and/or 5-FU treatment altered the cell cycle and increased cell death in HCT116 cells.....	51
F. 6-AN and/or 5FU treatment altered the cell cycle and increased cell death in HCT116 p53 <sup>-/-</sup> .....	54
G. 6-AN and/or 5-FU treatment induced ROS generation .....	55
H. 6-AN and/or 5-FU treatment increased GPx activity .....	56
V- DISUCSSION.....	58
REFERENCES .....	65

## ILLUSTRATIONS

Figure	Page
1. Global Estimation Numbers of the Different Types of Cancer Cases and Deaths.....	1
2. Genetic and Histological Changes During Colorectal Cancer Development.....	4
3. Mechanism of Action of 5-FU in a Neoplastic Cell.....	6
4. The Hallmarks of Cancer .....	8
5. Metabolic Pathways in Tumor Cells .....	9
6. The Pentose Phosphate Pathway .....	11
7. Glutathione Reductase Reaction .....	13
8. Key Glycolytic and PPP Oncoproteins and Tumor Suppressor Proteins....	15
9. Total Dehydrogenase Basel Activity in CRC cells .....	16
10. Polydatin Mechanisim of Action in a Cancer Cell.....	17
11. Chemical Structure of 6-AN.....	19
12. G6PD mRNA Expression Levels in CRC .....	35
13. Effect of Polydatin Treatment on HCT116 Cells.....	36
14. Effect of DHEA Treatment on HCT116 Cells .....	37
15. Effect of 6-AN Treatment on HCT116 Cells .....	39
16. MTT versus SRB.....	40
17. 6-AN Treatment With and Without Replenishment.....	41
18. Effect of Polydatin/5-FU Combination Treatment on HCT116 cells .....	43

19. Effect of DHEA/5-FU Combination Treatment on HCT116 Cells.....	44
20. Effect of 6-AN/5-FU Treatment on HCT116 Cells.....	46
21. Effect of 6-AN and/or 5-FU Treatments on different CRC cell lines .....	47
22. G6PD Protein Expression and Activity Levels Upon 6-AN and/or 5-FU Treatment on Different CRC Cell Lines.....	49
23. Transketolase Protein Expression in HCT116 Cells Upon 6-AN and/or 5-FU Treatment .....	50
24. Cell Cycle Distribution of HCT116 cells Upon 6-AN and/or 5-FU Treatment.....	52
25. Effect of 6-AN and/or 5-FU Treatment on Different Cellular Proteins in HCT116 Cells .....	53
26. Cell Cycle Distribution of 6-AN and/or 5-FU Treated HCT116 p53 <sup>-/-</sup> Cells.....	55
27. Effect of 6-AN and/or 5-FU Treatment of ROS generation in HCT116 Cells Using NBT Assay.....	56
28. Effect of 6-AN and/or 5-FU treatment on GPx Activity in HCT116 Cells	57

## TABLES

Table	Page
1. Comparison Between Different Oxidative PPP Inhibitors .....	21
2. Polydatin and 5-FU Compusyn Synergy Study .....	43
3. DHEA and 5-FU Compusyn Synergy Study .....	45
4. 6-AN and 5-FU Compusyn Synergy Study .....	46

## ABBREVIATIONS

$\delta$ -H2AX	phosphorylated H2A histon family member X
°C	Celsius
$\mu$ g	Microgram
$\mu$ L	Microliter
$\mu$ M	Micromolar
5-FU	5-Fluorouracil
6-AN	6-aminonicotinamide
6-PG	6-Phosphogluconate
6-PGD	6-Phosphogluconate Dehydrogenase
6ANAD	6-aminonicotinamide adenine dinucleotide
6ANADP	6-aminonicotinamide adenine dinucleotide phosphate
AKT	protein kinase B
APC	Adenomatous Polyposis Coli
BAX	BCL-2 Associated X Protein
BCL-2	B-cell Lymphoma 2
CDK	Cyclin-dependent Kinase
CI	Combination Index
CIMP	CpG Island Methylator Phenotype
CIN	Chromosomal Instability

CRC	Colorectal Cancer
DHEA	Dehydroepiandrosterone
DMSO	Dimethyl Sulfoxide
EGF	Epidermal Growth Factor
ELISA	Enzyme-Linked Immunosorbent Assay
F6P	Fructose 6 Phosphate
FAP	Familial Adenomatous Polyposis
FBS	Fetal Bovine Serum
G6P	Glucose 6 Phosphate
G6PD	Glucose 6 Phosphate Dehydrogenase
GLUT1/4	Glucose Transporter 1/4
GPx	Glutathione Peroxidase
GR	Glutathione Reductase
GSH	Glutathione
GSSG	Oxidized Glutathione
HBV	Hepatitis B Virus
HMP	Hexoses Monophosphate Shunt
KOH	Potassium Hydroxide
M	Molar
mg	milligram
mg/ml	Milligram per milliliter
MMP-1	Metalloproteinase-1

MSI	Microsatellite Instability
mTOR	mammalian target of rapamycin
MTT	3-(4,5-Dimethylthiazol-2-yl)-2,5-Diphenyltetrazolium Bromide
NADH	Nicotinamide Adenine Dinucleotide
NADPH	Nicotinamide Adenine Dinucleotide Phosphate
NBT	Nitroblue Tetrazolium
NO	Nitric Oxide
nm	Nanometer
NP-40	Nonidet P-40
O.D.	Optical Density
PARP	Poly (ADP-ribose) Polymerase
PBS	Phosphate Buffer Saline
PI	Propidium Iodide
PI3K	phosphoinositide 3-kinase
PMI	Phosphomannose Isomerase
PPP	Pentose Phosphate Pathway
R5P	Ribose 5 Phosphate
Redox	Reduction-oxidation
ROS	Reactive Oxygen Species
rpm	Rotations per minute
Ru5P	Ribulose 5 phosphate
SD	Standard Deviation

SEM	Standard Error of the Mean
SRB	Sulforhodamine B
TALDO	Transaldolase
TCA	Tricarboxylic Acid
TIMP-1	Tissue inhibitor of metalloproteinase-1
TKT	Transketolase
TS	Thymidylate Synthase
U/ml	Units per mililiter
Xu5P	Xylulose 5 Phosphate



# CHAPTER I

## INTRODUCTION

### A. Colorectal Cancer

#### a. Incidence and Statistics

Colorectal cancer (CRC) is a type of cancer that affects the colon or the rectum. It is the third most common cancer and the second cause of cancer-related deaths after cardiovascular diseases worldwide. In 2018, the World Health Organization estimated that there were 1.8 million cases and 862,000 deaths from CRC (Figure 1) (WHO, 2018). Over one hundred thousand cases are estimated to be diagnosed in the United States (Siegel et al., 2020) It is the second most common cancer in women and the third most common cancer in men (WCRF, 2018). In Lebanon, data collected between 2003 and 2008 showed similar results, whereby there were 15.3 and 14.1 cases of CRC per 100,000 people for men and women, respectively (Shamseddine et al., 2014).

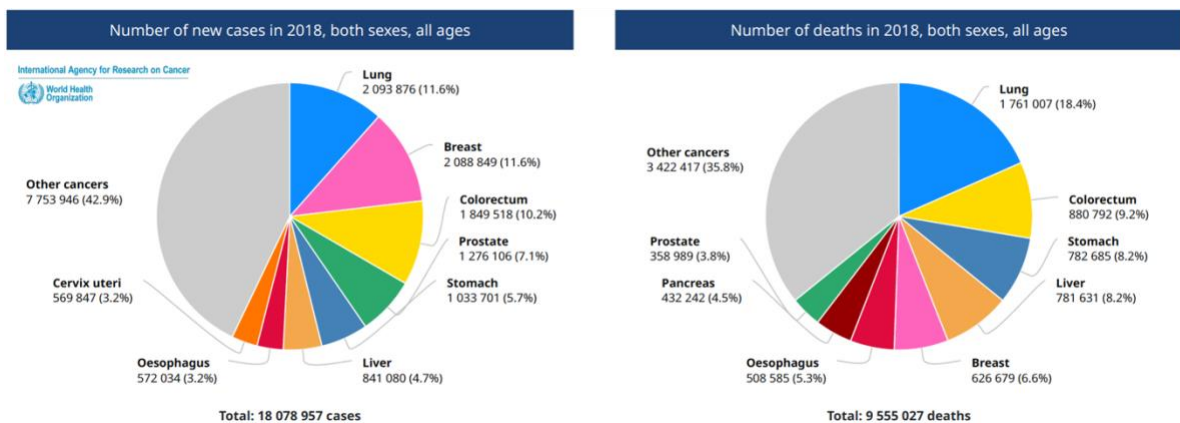


Figure 1. Global estimation of the numbers of the different types of cancer cases and deaths worldwide, for all sexes, and all ages in 2018. CRC is the third most common cancer and the second cause of cancer-related death (WHO 2018).

### ***b. Colorectal Cancer Risk Factors, Symptoms, Diagnosis, and Prognosis***

The risk factors of developing CRC include modifiable and unmodifiable risk factors. While age (over 65 years old) and family history are uncontrollable factors, other life-style risk factors such as smoking, alcohol consumption, diet, body mass index, and physical activity are modifiable risk factors (Oines et al., 2017). Additionally, a personal history of inflammatory bowel disease including ulcerative colitis and Crohn's disease increase a patient's risk in developing CRC (Marmol et al., 2017). Furthermore, a growing body of evidence suggests that the dysbiosis of the gut microbiome is a component influencing the multistep process of cancer development (Montalban-Arques et al., 2019). The signs and symptoms of CRC depend on the sight of the cancer in the colon or the rectum and include abdominal discomfort, changes in stool caliber, gastrointestinal bleeding, and fatigue. Screening for adenomatous polyps in the large intestine is used as a mean to identify CRC. Invasive screening modalities include colonoscopy, sigmoidoscopy, and computed tomographic colonography. Non-invasive detection methods include the fecal immunochemical and fecal occult blood tests and stool DNA testing (Nee et al., 2020). Another non-invasive advanced method for the genomic profiling of tumors is the use of next generation sequencing technology on circulating tumor DNA derived from blood or liquid biopsies of cancer patients. This allows for the evaluation of the molecular characteristics and makeup of the tumor (Schwaederle et al., 2017). The five-year survival rate of CRC in patients with localized tumors is 90%, however, only 39% of patients are diagnosed at this early stage. The general five-year survival rate is 39% (ACS, 2020).

### ***c. Molecular Pathogenesis of Colorectal Cancer***

Colorectal cancer can be classified as sporadic (70%), inherited (5%), and familial (25%) (Marmol et al., 2017). The disease has a heterogeneous etiological background. It develops as a result of the sequential acquisition of genetic and epigenetic modifications that inactivate tumor-suppressor genes, activate oncogenes, and alter DNA repair mechanism genes. Normal colorectal epithelial tissue is morphologically transformed into benign polyps through the stepwise process of successive accumulation of mutations overtime. Polyps are adenomatous neoplastic lesion precursors that some might evolve into a carcinoma state over an estimated 10-15-year period (Figure 2) (Vogelstein et al., 2013).

Globally, there are three major distinct mechanisms that can lead to CRC, namely chromosomal instability (CIN), microsatellite instability (MSI), and CpG island methylator phenotype (CIMP). Chromosomal instability is the most common abnormality in sporadic CRCs (70-90%) and is also referred to as the traditional adenoma-carcinoma pathway. This instability is typically initiated by mutations in the adenomatous polyposis coli (APC) followed by *RAS* activation and loss of heterozygosity or function of the crucial tumor suppressor *p53* gene, whereby, *p53* is a key regulator of cell proliferation, apoptosis, and cell cycle checkpoint. Conversely, the epigenetic CpG island methylation phenotype (10-20%) is characterized by the abnormal methylation of cancer-related genes thus leading to genetic silencing or overactivation. This pathway is associated with *RAS* and *RAF* mutations (Dekker et al., 2019).

Hereditary CRC can be subdivided into polyposis and non-polyposis (Lynch syndrome and familial CRC) cancers. The familial adenomatous polyposis (FAP) variant is involving multiple polyps in the colon. Lynch syndrome is characterized by the expansion

or contraction of microsatellite regions in the tumor, which is caused by defects in the DNA mismatch repair system genes, such as *MLH1* and *MSH2* genes (Nguyen et al., 2018).

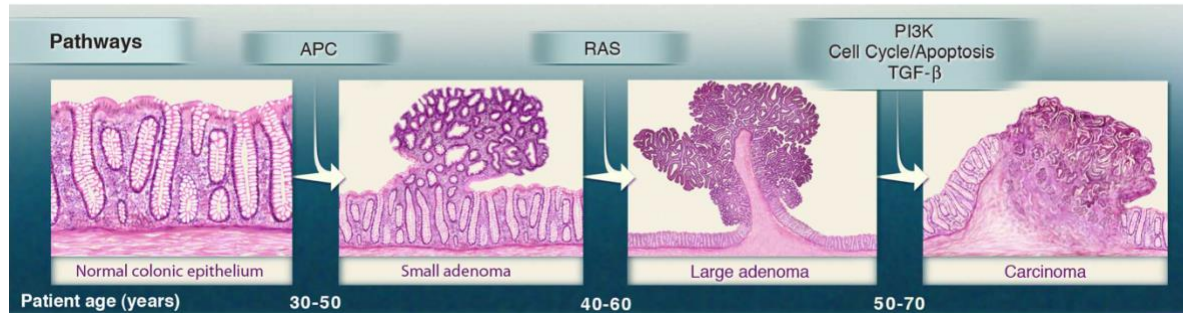


Figure 2. Genetic and histological changes during colorectal cancer development. Driver mutations mostly appear in the APC gene followed by second and third round hit that expand tumor tissue (Vogelstein et al., 2013).

#### *d. Therapy of Colorectal Cancer*

The treatment of CRC depends on the stage of diagnosis. For the early stages of the disease the cancer will have either only invaded locally (stage I-II) or with regional lymph-node metastases (stage III). Surgery is the mainstay therapy for these patients.

Alternatively, patients may undergo endoscopic resection of polyps as the source of management to remove the neoplastic tissue. Metastatic CRC (stage III-V) patients usually present with more advanced and unresectable tumors (Dekker et al., 2019). Therefore, adjuvant radiotherapy, systematic chemotherapy, and/or targeted therapeutic regimens are generally required (Punt et al., 2017).

Fluoropyrimidine-based chemotherapy, mainly 5-Fluorouracil (5-FU), is considered the backbone of first-line metastatic CRC treatment. It can be received as a single-agent therapy or improved with combination regimens containing other cytotoxic drugs, such as oxaliplatin and irinotecan. However, chemotherapy is associated with certain limitations

such as systematic toxicity, low tumor-specific selectivity, and acquired resistance. Hence this lead to the emergence of monoclonal antibody-targeted therapy that inactivates cancer cells directly by inhibiting various cell proliferation and migration pathways. Some of the first food and drug administration (FDA) approved drugs for targeted CRC therapy are cetuximab (anti-EGFR) and bevacizumab (anti-VEGF). Targeted therapy can be used in conjunction with first-line chemotherapy or as a second-line of treatment (Ciombor et al., 2015). In addition, advances in immunotherapy are being made that enhance immune recognition pathways against cancer cells (Kruger et al., 2019). Since cancer cells harbor various genetic and epigenetic modifications, tumor cells can be identified and obliterated by the host immune system through activation of T cells to bind to major histocompatibility complex of antigen-presenting cells. Microsatellite instability-high patients have a high mutational burden that results in many neoantigen with potential to be recognized by one's immune system (Kopetz, 2019).

#### 1- 5-Fluorouracil Resistance

5-FU is an S-phase inhibitor fluorinated pyrimidine analogue antimetabolite drug used worldwide for the treatment of metastatic CRC (De Angelis et al., 2006). 5-FU works by inhibiting the rate-limiting nucleotide synthetic enzyme thymidylate synthetase (TS), the sole *de novo* source of thymidine. It also acts by misincorporation into the DNA and RNA structures thus disrupting RNA processing and blocking cell proliferation (Longley et al., 2003) (Figure 3). Although 5-FU improves overall response in patients, unfortunately as high as 50% of metastatic CRC develop resistance to 5-FU based chemotherapy (Douillard et al., 2000; Giacchetti et al., 2000). Discovered mechanisms of resistance to 5-FU showed that its effect can be hindered at many levels, such as at the stage of drug influx and efflux,

its early metabolism and degradation by various enzymes, and resistance at the cell cycle kinetic and apoptotic levels (Mader et al., 1998). Similarly, data suggest that MSI-high patients lack benefit towards 5-FU-based chemotherapy compared to microsatellite-stable patients (Battaglin et al., 2018).

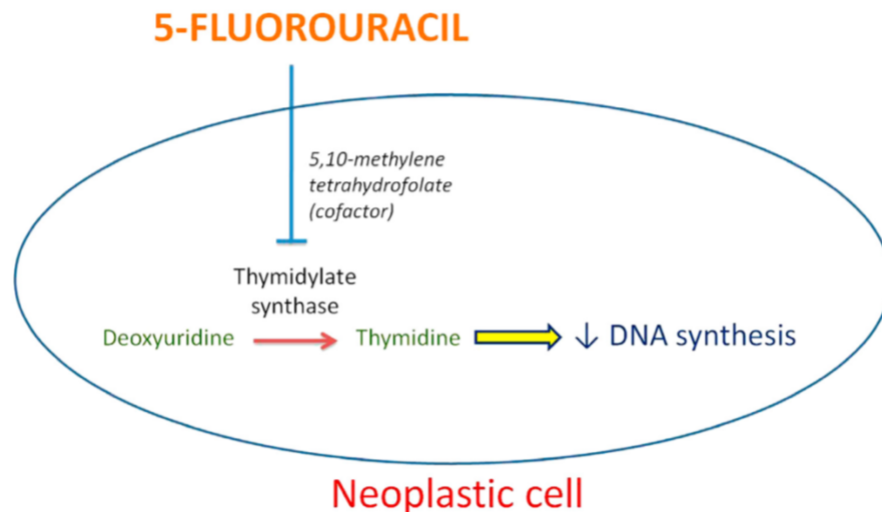


Figure 3. Mechanism of action of 5-FU on a neoplastic cell. 5-FU inhibits the action of Thymidylate synthase by binding to its cofactor site. Thus, it reduces DNA synthesis and replication (Micali et al., 2014).

## B. Cancer Metabolism

### a. Overview

Cancer cells rewire their metabolism to generate sufficient levels of cellular components to support cell proliferation. The hallmarks of cancer establish an organizational principle for explaining the complexities during the multistep process of tumorigenesis. The hallmarks include resisting cell death, sustaining proliferative signaling, evading growth suppressors, enabling replicative immortality, activating invasion and metastasis, inducing angiogenesis, avoiding immune destruction, and reprogramming

cellular energetics (Figure 4) (Hanahan et al., 2011). The last two hallmarks emerged in 2011 and have been drawing a growing amount of attention since. Interest in targeting metabolic pathways in cancer has been renewed over the past decade. The higher rates of energy metabolism involve the alteration of protein, lipid, carbohydrate, and nucleic acid metabolism (Figure 5). The abnormal tumor microenvironment induces stressors such as hypoxia, low pH, and nutrient deprivation, elicit to cancer metabolism alteration, including autophagy (Cairns et al., 2011).

The uncontrolled proliferation of cancer cells demands an increased import of building blocks that support tumor progression. Glucose and glutamine, the principle growth-supportive substrates, provide intermediates that are diverted into branching pathways for numerous biosynthetic precursors. These nutrients fuel ATP generation and produce nicotinamide adenine dinucleotide (NADH) and nicotinamide adenine dinucleotide phosphate (NADPH). Furthermore, these precursors assist in assembling nucleotide and non-essential amino acids as well as supporting fatty acid and organelle biosynthesis (Martinez-Outschoorn et al., 2017). First in the series of the routs that branch from glycolysis is the pentose phosphate pathway (PPP), a reducing anabolic pathway essential for neoplastic transformation. Tumor cells aberrantly activate oncogenes and/or repress tumor suppressor genes that lock cancer cells in a constitutively scavenging state. Notably, the RAS and phosphoinositide 3-kinase (PI3K)/ protein kinase B (AKT)/ mammalian target of rapamycin (mTOR) signaling pathway offer restorative overexpression of the plasma membrane glucose transporter 1 (GLUT1) along with the first enzyme of glycolysis, hexokinase (Pavlova et al., 2016). This marked increase in consumption of glucose by tumors compared to healthy counterpart tissue is known as the Warburg effect. Under

aerobic conditions, normal cells metabolize glucose through glycolysis then further in the mitochondria through oxidative phosphorylation. Otto Warburg observed that in most cancer cells, even in the presence of oxygen, tumor cells favor and reprogram their glucose metabolism to rely largely on glycolysis for energy production, resulting in a state of “aerobic glycolysis” (Bader et al., 2020).

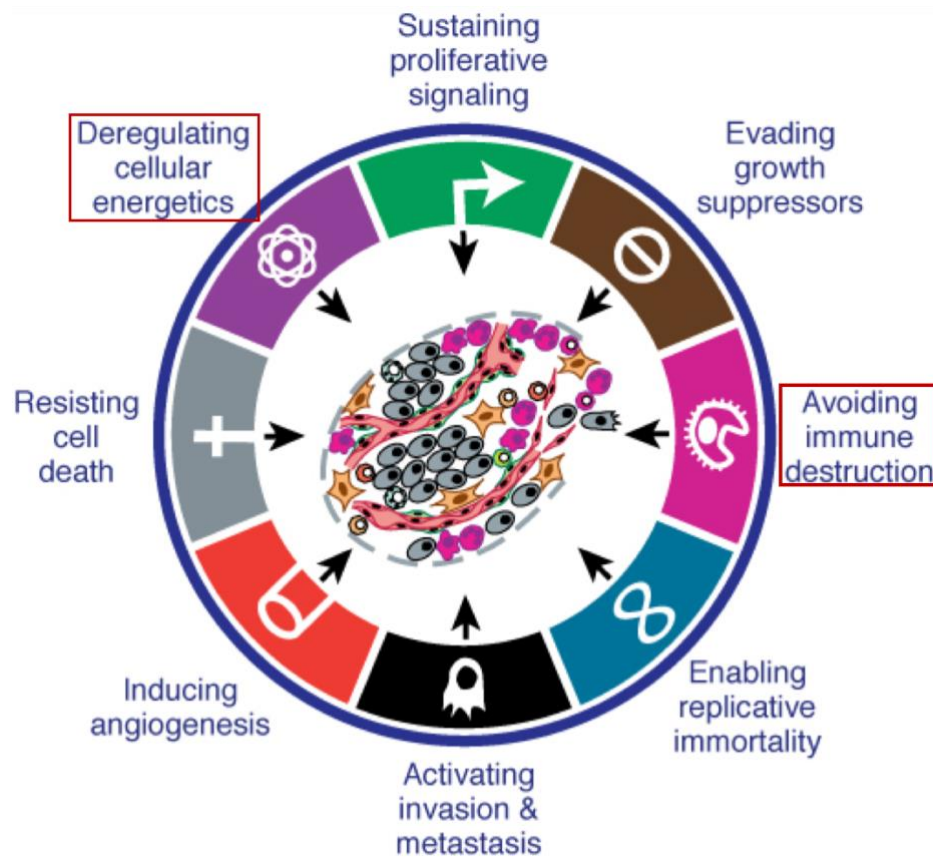


Figure 4. The eight acquired capabilities that constitute the hallmarks of cancer. Neoplastic cells acquire progressive functional capabilities during the pathogenesis. The latest two hallmarks, relating to cancer metabolism and immunotherapy, emerged in 2011 and have been gaining widespread interest since (Hanahan et al., 2015)



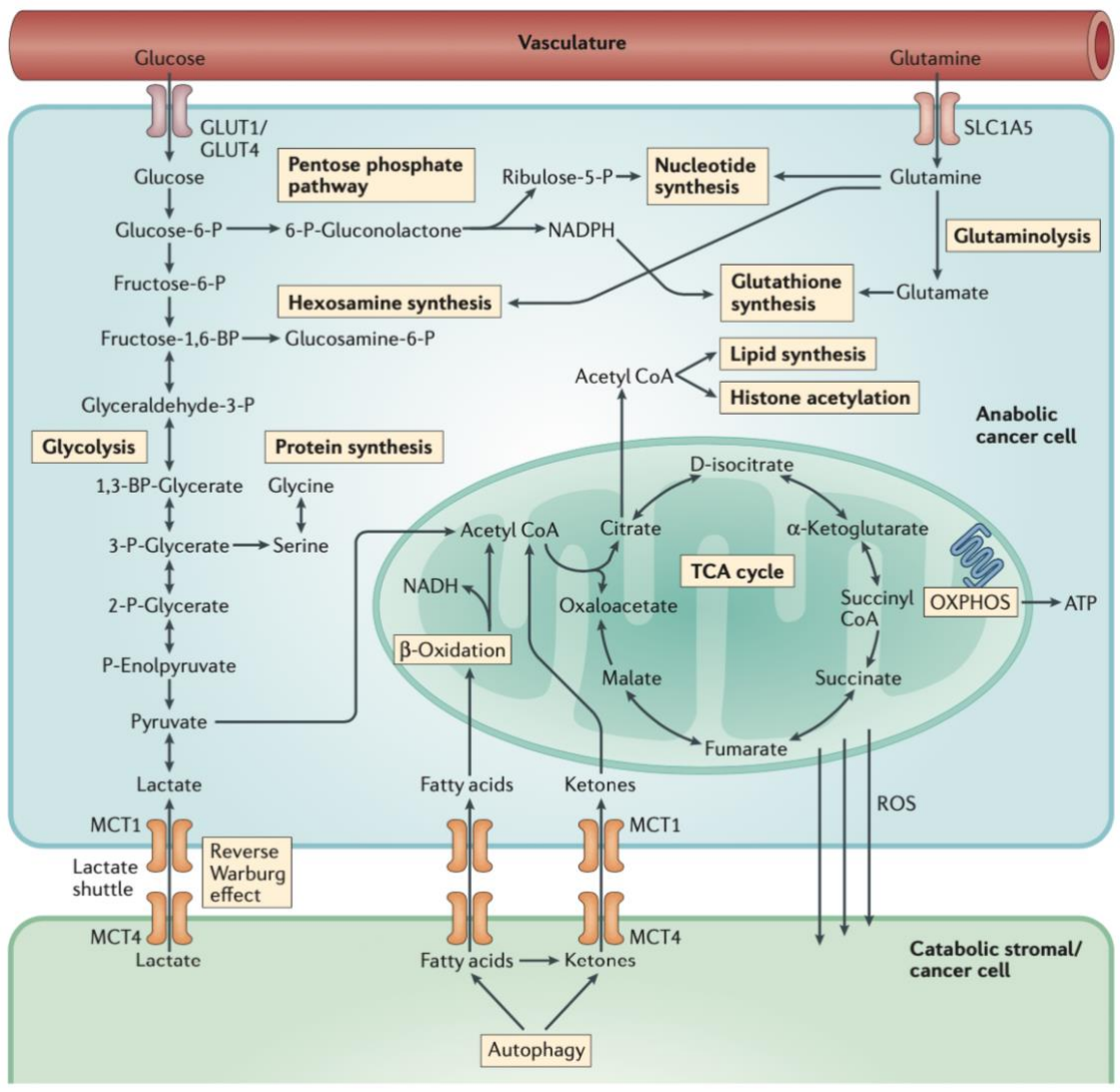


Figure 5. The metabolic pathways comprised in a tumor cell. Cancer cells utilize big amounts of glucose and glutamine. Multiple interconnected metabolic coupling supports the incorporation of various precursors into anabolic routs to synthesize ATP, nucleotides, NADPH, proteins, and lipids for continuous growth (Martinez-Outschoorn et al., 2017)

***b. The Pentose Phosphate Pathway***

The PPP, also known as the hexoses monophosphate shunt (HMP) or the phosphogluconate pathway, is a pivotal elevated pathway in neoplasms (Figure 6). It contributes to ribonucleotides synthesis and maintains cytosolic reduction-oxidation

(redox) balance through NADPH production. Glucose 6 phosphate dehydrogenase (G6PD), the first and rate-limiting PPP enzyme, gained significant interest when discovered to be correlated with hemolytic anemia, a condition induced by oxidizing agents such as fava beans. Moreover, red blood cells are rendered vulnerable as the PPP is the singular source of NADPH production for protecting them from reactive oxygen species (ROS) damage (Patra et al., 2014). With over 400 million people suffering from genetic defects in G6PD, it is interesting to study its correlation with a lower risk of CRC, which calls into question whether this confers a selective growth advantage in these patients (Dore et al., 2016). Collectively, the PPP maintains redox homeostasis and reduced nitrogenous bases. It shuttles intermediates with tricarboxylic acid (TCA), lipid, and amino acid metabolism depending on the cellular demand. The PPP is divided into two interrelated phases: the irreversible oxidative phase and the reversible non-oxidative phase.

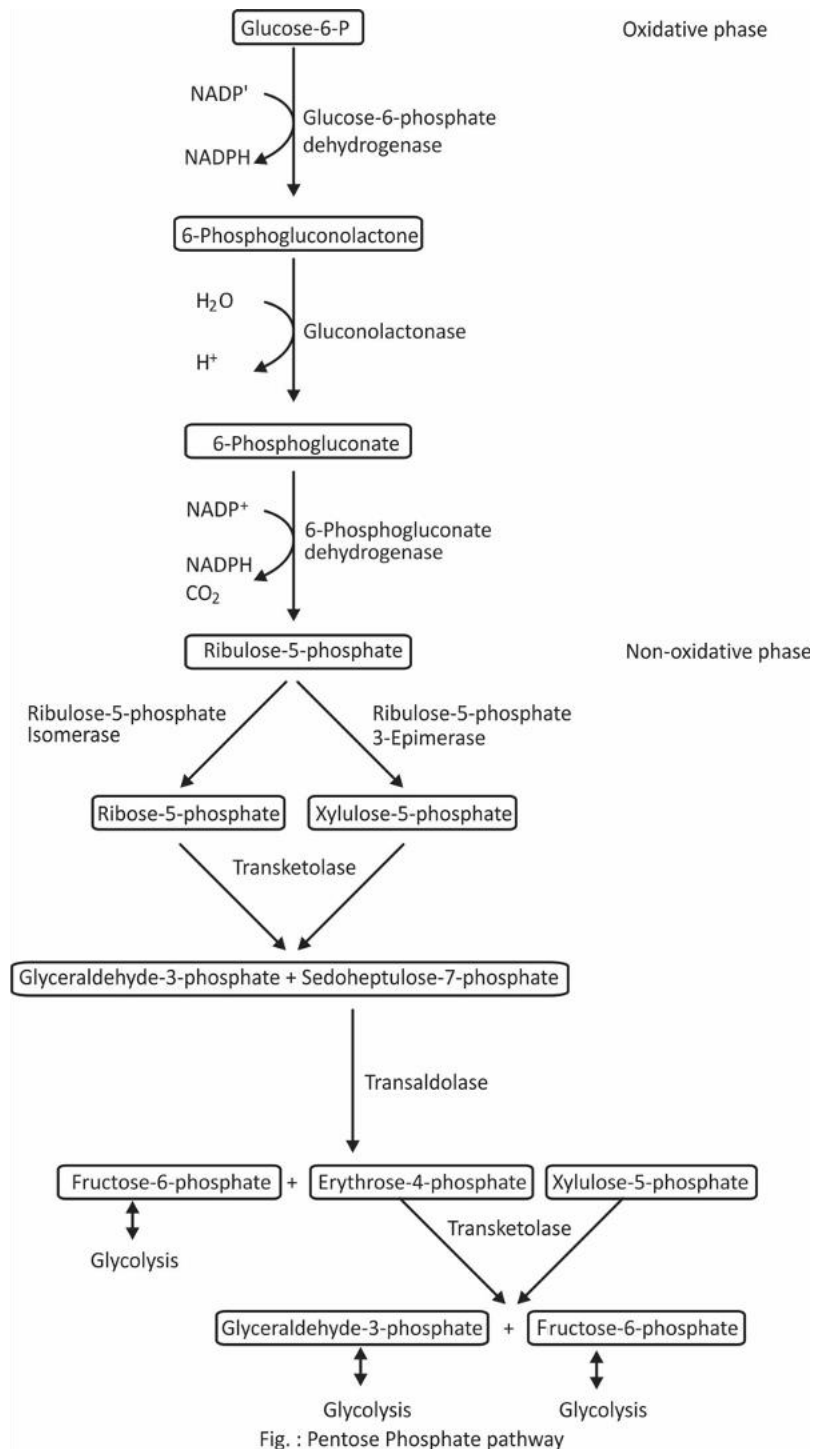


Figure 6. The pentose phosphate pathway. It has two phases: oxidative and non-oxidative. The main product of the first phase is NADPH, and that of the second part is Ribulose 5 Phosphate. Glucose 6 Phosphate, Fructose 6 Phosphate, and Glyceraldehyde 3 Phosphate circulate with glycolysis (Let's Talk Academy, 2018)

## 1- The Oxidative Phase

This pathway goes through dehydrogenation, hydrolyzation, and decarboxylation steps to generate 2 NADPH molecules and a ribose. The primary substrate, glucose 6 phosphate (G6P), is oxidized to 6-phosphogluconate (6PG) by G6PD, yielding an NADPH molecule. Then, 6PG undergoes oxidative decarboxylation by 6-phosphogluconate dehydrogenase (6PGD) to produce ribulose 5 phosphate (Ru5P) and a second NADPH molecule. Being a critical enzyme, the expression and activity of G6PD are tightly regulated. In rapidly proliferating cells, a high NADP<sup>+</sup>/NADPH ratio positively regulates G6PD to support NADPH production. Additionally, G6PD can be extrinsically regulated by some oncogenes such as platelet-derived growth factor (PDGF), epidermal growth factor (EGF), PI3K, and RAS (Patra et al., 2014), whereas p53 was reported to be a negative regulator of G6PD by binding directly to it, preventing monomer dimerization (Peng Jiang et al., 2011). 6PDG has frequently been studied with G6PD for its pivotal role in tumorigenesis. In fact, 6PDG genetic silencing revealed p53 accumulation and senescence of lung cancer cells, and slowed tumor growth in mouse xenograft models (Sukhatme et al., 2012). Moreover, enhanced G6PD activity was reported in papillary thyroid carcinoma, colorectal, renal, and prostate cancer. NADPH is an essential anabolic reducing agent that supports reductive biosynthesis of fatty acids and nucleotides. Furthermore, NADPH maintains survival under oxidative stress conditions that are generated from deregulated mitochondria or metabolically active cells (Kowalik et al., 2017). Moreover, glutathione (GSH) is an essential antioxidant tripeptide that scavenges ROS, and NADPH is a critical cofactor involved in continuously replenishing the glutathione reductase pool (Figure 7) (Pai et al., 1983).

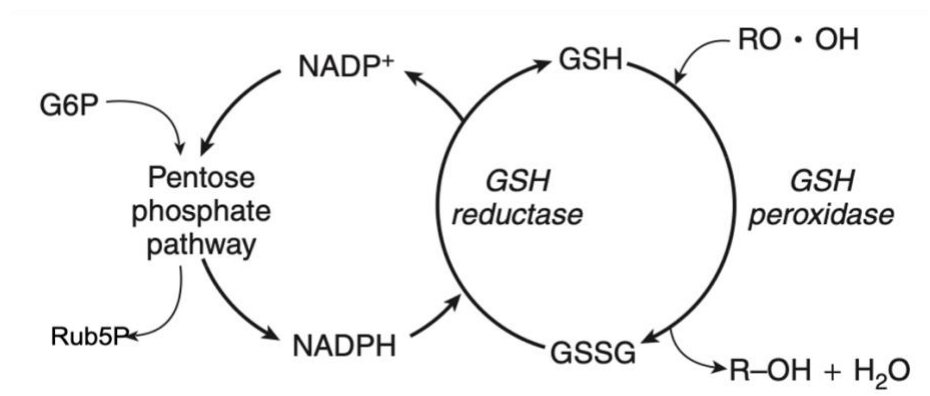


Figure 7. NADPH produced from G6PD is an essential cofactor in reducing glutathione. Glutathione is oxidized to GSSG to protect cells from ROS derivatives and free radicals (Rudd, 2012).

## 2- The Non-Oxidative Phase

The recycling phase starts with Ru5P that is converted into the anabolic pentose sugar ribose 5 phosphate (R5P), a structural component for purine and pyrimidine nucleotides biosynthesis. Xylulose 5 phosphate (Xu5P) was reported to increase glycolytic flux. The major enzymes that lead the non-oxidative PPP are transketolase (TKT) and transaldolase (TALDO). The reversible nature of these enzymes allows glycolytic intermediates, such as fructose 6 phosphate (F6P) and glyceraldehyde 3 phosphate (GA3P), to be recruited into this pathway and vice versa (Patra et al., 2014). Overexpression of TKT has been associated with tumor invasiveness and poor cancer prognosis in colon and urothelial cancers (Langbein et al., 2006; Patra et al., 2014).

## 3- Regulation

PPP enzymes can be allosterically regulated by their own metabolic products to maintain expression and facilitate growth. Depending on the need, the PPP can operate in different modes. In rapidly dividing cells, TKT and TALDO reversely channel GA3P and

F6P from glycolysis to the non-oxidative PPP to generate RNA and DNA precursors from R5P. During oxidative stress, F6P is converted back to G6P through glycolysis and shuttled back to the PPP to maintain NADPH homeostasis. On the other hand, when ATP is in higher demand, PPP products can be circulated back into the glycolytic pathway (P. Jiang et al., 2014). When glucose availability is scarce, pathways other than the PPP maintain NADPH thresholds to prevent cell death. One of these mechanisms is mediated by the activation of AMP-activated protein kinase (AMPK) that halts the consumption of NADPH by fatty acid synthesis. Rather, the malic enzyme and isocitrate dehydrogenase induce fatty acid oxidation which generates more NADPH molecules (Patra et al., 2014).

### *c. Pentose Phosphate Pathway Deregulation in Cancer Metabolism*

Cancer cells can overcome strict metabolic surveillance of the PPP by acquiring genetic mutations and epigenetic modifications that impact this pathway. In addition to stimulating the expression of p53-induced glycolysis and apoptosis regulator (TIGAR), p53 can repress transcription of GLUT1 and GLUT4. TIGAR functions as a fructose 2,6 biphosphate phosphatases, which inhibits phosphofructose kinase, thereby redirecting glycolytic intermediates towards the PPP (Galluzzi et al., 2013). P21-activated kinase 4 (PAK4) promotes glucose uptake, NADPH production, and lipid biosynthesis. It positively correlated with CRC in tissue samples as it binds to G6PD and over activates it (X. Zhang et al., 2017). mTOR complex 1 is frequently activated in cancer cells (Figure 8). Its activation revealed a significant upregulation in the oxidative PPP, mainly G6PD, by elevating the activity of transcription factor sterol regulatory element-binding protein (SREBP) (Duvel et al., 2010).

We and others have shown the activity of oxidative phase PPP enzymes to be upregulated in CRC (Figure 9) (Al Saleh et al., 2018). Shibuya et al. showed that the synthesis of G6PD and TKT enzymes were augmented in CRC patients (Shibuya et al., 2015) while Shimizu et al. published similar findings in hepatocellular carcinoma specimens (Shimizu et al., 2014). In a pancreatic cancer mouse model, K-Ras stimulation was shown to activate the non-oxidative phase of the PPP (Ying et al., 2012). Thus, exploiting the reprogrammed metabolic differences between tumor and healthy cells holds promises as novel therapeutic approaches that selectively target cancer cells (Martinez-Outschoorn et al., 2017).

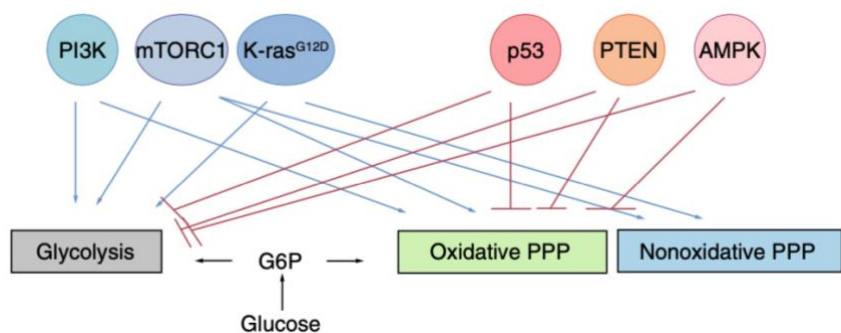


Figure 8. Key glycolytic and PPP oncoproteins and tumor suppressor proteins that regulate metabolic flux between the pathways (P. Jiang et al., 2014).

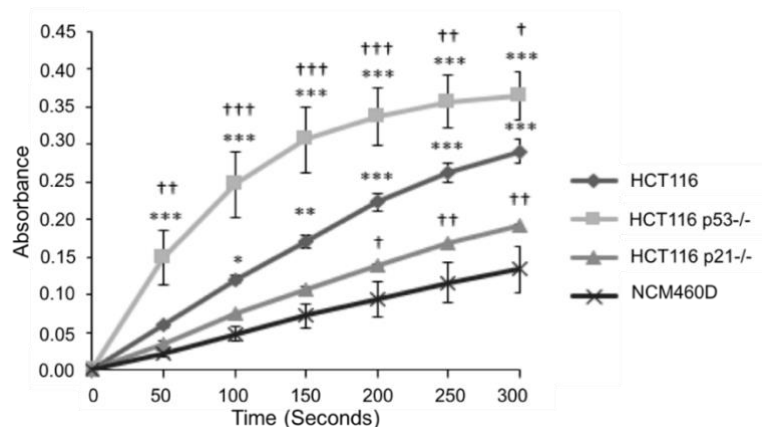


Figure 9. Comparison of total dehydrogenase basal activity of the PPP in human colorectal cancer cells (HCT116, HCT p53<sup>-/-</sup>, HCT116 p21<sup>-/-</sup>) and the normal-like NCM460D cells (Al Saleh et al., 2018)

### C. Pentose Phosphate Pathway Inhibitors

The PPP influx correlates with malignancy and tumor invasion, and its inhibition remains an attractive research approach against cancer. Unfortunately, efficient anti-PPP agents are still not available in the clinical setup and investments are still needed. Listed below are a set of synthetic and natural oxidative PPP inhibitors, namely inhibitors of G6PD and 6PGD, that could be used to treat CRC and restore sensitivity to chemotherapy.

#### a. Polydatin

Polydatin, (3,4',5-trihydroxystilbene-3- $\beta$ -D-glucoside; trans-resveratrol 3- $\beta$ -mono-D-glucoside; piceid), is a glucoside of resveratrol extract from the Chinese herb *Polygonum cuspidatum*. It is abundantly found in other plants such as grapes, peanuts, and cocoa-containing products. It has many biomedical properties such as cardioprotective activity, anti-inflammatory, immunomodulatory, and antioxidative effects (Du et al., 2013).



Additionally, it has apoptotic characteristics in neoplastic cells through direct inhibition of G6PD enzymatic activity and impairing NADPH production (Figure 10). In head and neck squamous cell carcinoma cells, polydatin was shown to increase ROS, endoplasmic reticulum stress, and apoptosis while arresting the cell cycle and inhibiting invasion. In an *in vivo* tongue cancer model, it shrank tumor size while inhibiting lymph node metastasis (Mele et al., 2018). Moreover, polydatin revealed a synergistic effect with Lapatinib, a tyrosine kinase inhibitor in breast cancer cells, by inducing autophagy (Mele et al., 2019). In CRC, polydatin was shown to induce cell-specific differentiation and apoptosis (De Maria et al., 2013). Currently, polydatin is in phase II clinical trials and was shown to have minimal side effects and high tolerance in humans (40 mg twice per day for 90 days) making it a natural favorable treatment (Cremon et al., 2017). Admittedly, the definitive target proteins and mechanism of action of polydatin remain undetermined.

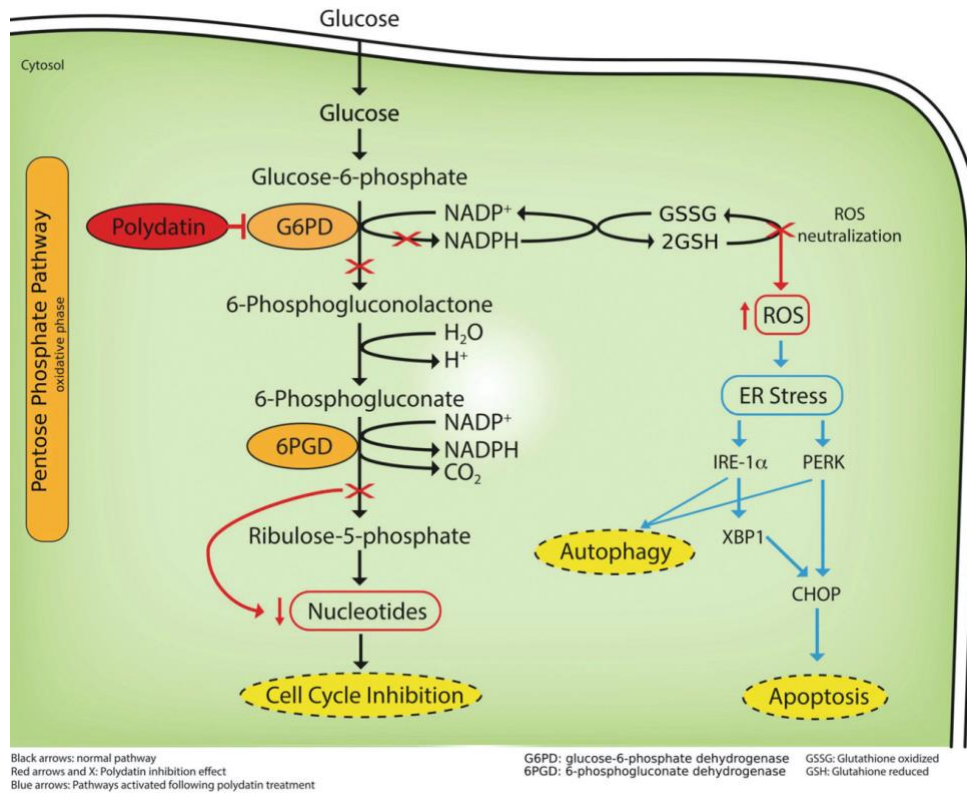


Figure 10. Schematic representation of polydatin in action in a cancer cell (Mele et al., 2018)

### b. Dehydroepiandrosterone

The discovery of the metabolic pathway of Dehydroepiandrosterone (DHEA) won the Nobel Prize in 1939 (Klinge et al., 2018). DHEA, (3 $\beta$ -hydroxy-5-androsten-17-one), is a 19-carbon endogenous hormone synthesized *de novo* from cholesterol in the adrenal gland. This steroid is a precursor for estrogen and androgen (Di Monaco et al., 1997). Together with its sulfur ester DHEA-S, they make up the most abundant steroid in the body and peak during the second and third decade of life (Klinge et al., 2018). However, DHEA is a hundred times more potent G6PD inhibitor (Di Monaco et al., 1997).

DHEA was originally found to employ a chondroprotective role and effective against osteoarthritis. It exerts a beneficial effect on osteoarthritic cartilage by positively modulating the balance between anabolic and catabolic signaling pathways. DHEA increased the expression of the tissue inhibitor of metalloproteinases-1 (TIMP-1) while it inhibited the expression and protein synthesis of metalloproteinases-1 (MMP-1). It was also found to suppress pro-inflammatory cytokines and inhibit atherosclerosis (Huang et al., 2018). Epidemiological analysis showed an inversely proportional correlation between serum DHEA levels and risk of developing breast hyperplasia (Zumoff et al., 1981).

Besides its natural hormonal role, research suggests that it is a potent inhibitor of mammalian G6PD. DHEA uncompetitively binds to both G6P and NADP<sup>+</sup>, where DHEA adheres to the enzyme-coenzyme-substrate ternary complex, however other studies show DHEA to be a noncompetitive G6PD inhibitor (Fang et al., 2016). It decreases cellular NADPH and increases ROS production (Gordon et al., 1995). DHEA studies showed that it was able to reduce G6PD activity in preneoplastic liver lesions and inhibit proliferation of CRC in soft agar assay (Kowalik et al., 2017). DHEA is, however, rapidly converted into other steroid hormones *in vivo* which renders its efficacy as an inhibitor of the oxidative PPP disputable (Di Monaco et al., 1997). Clinical trails of DHEA are encumbered by the high oral doses required and, therefore, DHEA is still in early development.

### *c. 6-Aminonicotinamide*

6-aminonicotinamide (6-AN) (Figure 11) is a monocarboxylic acid amide that is the most potent antagonist of niacin. This antimetabolic drug is activated when it is converted into the respective analogs of NAD<sup>+</sup> and NADP<sup>+</sup>, with NADP<sup>+</sup> being converted into 6-

aminonicotinamide adenine dinucleotide phosphate (6ANADP) much faster and more completely than NAD is converted into 6-aminonicotinamide adenine dinucleotide (6ANAD) (Herken, 1968). These analogs are incapable of participating as coenzymes in the redox reactions of the body (Carmona et al., 1990). Conversion of NAD and NADP into these corresponding analogs requires one of two possible mechanisms: (1) by 6-AN replacing the nicotinamide moiety of existing NAD and NADP in the reaction catalyzed by NAD(P) glycohydrolase. Alternatively, (2) by 6-AN being incorporated into these pyridine nucleotides during their *de novo* synthesis (Dietrich et al., 1958).

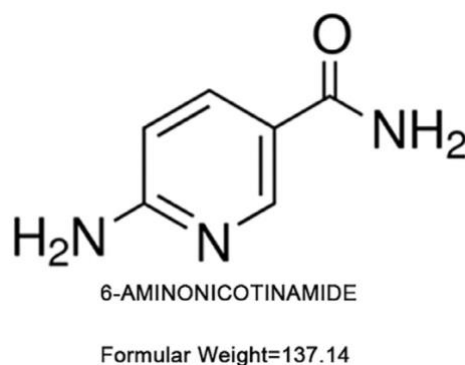


Figure 11. Chemical Structure of 6-AN (Ren et al., 2019)

6-AN acts as a competitive inhibitor of the NADP-dependent G6PD and 6-PDG enzymes, evidenced by 6-AN increasing the levels of ROS production while reducing NADPH biosynthesis (Budihardjo et al., 1998). The incubation of 6-AN with isolated hepatocytes (Carmona et al., 1990) and human lung carcinoma cells (Varnes, 1988) resulted in a marked buildup of 6PG levels. Preclinical trials have shown that the

application of 6-AN in adjuvant antineoplastic drugs serves to potentiate the effects of radiation and chemotherapy (Koutcher et al., 1993), as reported in mammary carcinoma mouse models (Kowalik et al., 2017). 6-AN induced an increase in the expression of the glucose-regulated stress protein (GRP78) and was found to be associated with enhanced responsiveness to DNA cross-linking agents in CRC (Belfi et al., 1999). Notably, the combination of cisplatin and 6-AN resulted in accumulation in platinum-DNA adducts (Budihardjo et al., 1998). Combining 6-AN with other drugs sensitizes treatment in distinct cancers such as breast, ovarian, leukemia (Stolfi et al., 1992), and hepatocarcinoma (Dietrich et al., 1968). In CRC, 6-AN was able to reverse the increase of G6PD and GSH as well as inhibited multidrug resistance in the doxorubicin-resistant human colon cancer cell line HT29-DX (Polimeni et al., 2011).

Additionally, 6-AN has cytotoxic and high antiviral activity, as evidenced in several cell lines and transgenic- hepatitis B virus (HBV) mouse models. Manifestly, 6-AN was able to inhibit the secretion of HBV surface antigen in hepatoblastoma cells through a reduction in the peroxisome proliferators-activated receptor- $\alpha$  (PPAR $\alpha$ ) transcription factor activity. Previous studies have also demonstrated its implication in treating skin diseases, namely psoriasis. 6-AN has antiparasitic responses against *Leishmania* and *Plasmodium falciparum* microorganisms (Ren et al., 2019).

Unfortunately, the clinical use of 6-AN is hampered by its toxicity at high concentrations, severe side effects, such as B-complex vitamin deficiency and serious neurological damage and paralysis presumably due to its direct action on the central nervous system (Penkowa et al., 2004). Therefore, further clinical research is still undergoing for identifying effective dosages of 6-AN administered to patients.

<b>Drug</b>	<b>Mechanism of action</b>	<b>Nature of the drug</b>	<b>Phase in clinics</b>
Polydatin	Natural inhibitor of G6PD	Glucoside of resveratrol	Phase II clinical trials (Mele et al., 2018)
DHEA	Non-competitive inhibitor of G6PD	Steroid hormone	On the market (Vassallo, 2019)
6-AN	Competitive inhibitor of G6PD and 6PGD	Monocarboxylic acid amide	Preclinical development (Zackheim, 1975) (Budihardjo et al., 1998)

Table 1. Comparison between different oxidative PPP inhibitors

***d. Combination therapies***

Researchers commonly use drug combinations to treat a range of diseases such as AIDS, bacterial infections, and cancer. Such combinations are less likely to be impeded by resistance and have the desirable potential to be synergistic. Synergistic combination therapies conceptualize that if lower doses of the principle agents can be used there can be dwindled toxicity (Torres et al., 2013). Chou-Talalay’s Compusyn software, a combination index algorithm, is a simple method for the quantitative assessment of synergistic and antagonistic drug combinations. The utilization of such algorithms is time-efficient, economical, and reduce the number of animals needed in an experiment or of patients needed in a clinical trial (Chou, 2010).

## CHAPTER II

### RATIONALE, SPECIFIC AIMS, AND SIGNIFICANCE

Colorectal cancer remains one of the deadliest cancers worldwide. Scientists have been massively investing in developing of new approaches to improve existing CRC chemotherapy (Xie et al., 2020). Cancer metabolism, a hallmark of cancer, is an emerging vulnerability of tumor cells, which offers a new therapeutic window for researchers to study (Hanahan et al., 2011). Glycolysis and the PPP enzymes are shown to be upregulated in CRC (Shibuya et al., 2015), and p53 is a crucial regulator. The latter inhibits the PPP by binding to the rate limiting enzyme, G6PD (Peng Jiang et al., 2011).

5-FU is the reference drug selected against CRC and is the most common chemotherapeutic treatment against solid tumors globally (Sara et al., 2018). However, drug-related toxicity and resistance are frequently seen in 5-FU treated patients. Therefore, combination treatments are often considered in CRC management. More recently, metastatic CRC protocols are considering combining 5-FU to other chemotherapeutic drugs (Sánchez-Gundín et al., 2018), but it is not known whether inhibiting the PPP sensitizes cells to 5-FU and whether 5-FU resistance in tumor cells is linked to PPP regulation.

We aim in this study to examine the different metabolic drugs that regulate the PPP in CRC and to determine whether they improve treatment outcomes in combination with current standard chemotherapy.

Accordingly we will use *in vitro* human CRC models harboring mutations relevant to colorectal tumorigenesis (mainly HCT116 and HCT116 p53<sup>-/-</sup>) and HCT116 5FU-R cells. In this study, we will characterize the potential treatment and investigate its

implications in various cellular processes involved in CRC progression and PPP upregulation. Specifically we will target the following aims:

- 1- Investigate the levels of *G6PD* expression in human normal and CRC tumors through *in silico* analysis.
- 2- Investigate the anti-tumor effect, modulation of metabolism, and the mechanism of action of several G6PD inhibitors, particularly, 6-AN, alone or in combination with 5-FU in human CRC *in vitro* models.
- 3- Assess the regulation of key PPP and related enzymes by 6-AN alone or in combination with 5-FU treatment.

Therefore, our hypothesis is that inhibiting the PPP in CRC may halt tumor progression and sensitize treatment to conventional chemotherapy. This research may lead to novel therapeutic strategies in CRC with drugs that target metabolism thus having implications in the future of clinical research.



## CHAPTER III

### MATERIALS AND METHODS

#### **A. *In Silico* Analysis of *G6PD* Expression**

Expression levels of *G6PD* mRNA were evaluated in publicly available datasets comprised of a wide collection of colorectal tumor versus normal counterparts. *In silico* analysis was conducted to investigate *G6PD* expression in malignant and premalignant (adenoma) lesions of the colon and rectum along with normal colon and rectal tissue. *P* values < 0.05 were considered statistically significant. The keywords used were CRC, *G6PD*, and *P*-value < 0.05, where the inclusion criteria included any significant study presenting *G6PD* mRNA expression in colorectal cancer vs. normal tissue. Particularly, data collected for our studies were obtained from (Hong et al., 2010), (Skrzypczak et al., 2010), (TCGA, 2011), and (Sabates-Bellver et al., 2007). Boxplots were obtained from the Oncomine website (Oncomine).

#### **B. Cell Culture**

##### ***1- In Vitro Human Model of Colorectal Cancer***

Human CRC cell lines: HCT116, HCT116 p53<sup>-/-</sup>, and HCT116 5-FU resistant (HCT116 5FU-R) were used in these studies.

##### **a. HCT116 Cell Line**

HCT116 is a well-characterized human epithelial adherent malignant cell line; one of three subpopulations of colonic carcinoma primary cell culture derived from an adult

male. HCT116 cells are highly motile, invasive, and tumorigenic in xenograph mouse models (Brattain et al., 1981). They can be used as a transfection host (Rajput et al., 2008). This cell line possesses a wild-type *p53* gene (Waldman et al., 1995). This cell line harbors a mutation in codon 13 of the *Ras* proto-oncogene and expresses the transforming growth factor beta 1 and beta 2. HCT116 is listed as CCL-247™ in the ATCC® cell bank and is considered as microsatellite instable cell line (Ahmed et al., 2013).

b. HCT116 5FU-Resistant Cell Line

HCT116 5FU-R CRC cell line was derived from the parental HCT116 cell line by incubating it with increasing concentrations of 5-FU (0.1 to 40  $\mu$ M), for a total period of eight months (Abdel-Samad et al., 2018). HCT116 5FU-R cells were regularly treated with 60  $\mu$ M of 5-FU the day after thawing without observing any effect on cell viability. A number of genes altered by 5-FU resistance were identified through microarray techniques, and include: alteration of nucleotide, amino acid, and oxygen metabolism, cytoskeletal organization, and transportation. Although 5-FU has been the reference drug for the last five decades, it is normally toxic and exhibits resistance in CRC patients (N. Zhang et al., 2008).

c. HCT116 p53<sup>-/-</sup> Cell Line

p53 protein is a major governor of the cell cycle, DNA repair mechanism, cell death and survival. More recently, p53 was shown to be a key regulator of cellular metabolism (Eriksson et al., 2017) and inhibits the PPP by binding to its rate limiting enzyme G6PD (Peng Jiang et al., 2011). Deregulated p53 is observed in 50 % of CRC patients and infers an aggressive and resistant behavior to chemotherapy (Li et al., 2015). This isogenic *in*

*in vitro* cell line has the same characteristics as HCT116 but *p53* was knocked out by homologous recombination. HCT116 *p53*<sup>-/-</sup> cells are relatively more resistant to drugs than their parental counterparts (Boyer et al., 2004).

## **2- Cell Culture Conditions**

HCT116 and HCT116 5FU-R cells were maintained in RPMI 1640 medium (Sigma-Aldrich) supplemented with 10% heat-inactivated fetal bovine serum (FBS, Sigma-Aldrich), 100 U/ml penicillin-streptomycin (Sigma-Aldrich) and 1 mM sodium pyruvate (Sigma-Aldrich). HCT116 *p53*<sup>-/-</sup> cells were maintained in DMEM (Sigma-Aldrich) media containing 10% FBS, 100 U/ml penicillin-streptomycin (Sigma-Aldrich), 1 mM sodium pyruvate (Sigma-Aldrich), and 1x MEM non-essential amino acid (Sigma-Aldrich). All cells were cultured in an incubator with 5% CO<sub>2</sub> at 37°C and under humidified conditions.

## **C. MTT Proliferation Assay**

HCT116 and HCT116 5FU-R cells were seeded in triplicates in a 96-well plate at a density of 5,000 cells/well, left overnight, and treated the next day using the below mentioned drugs. Cells were treated with a panel of Polydatin (Phytolab) concentrations with daily replenishment for up to 72 hours. Cells exposed with different concentrations of DHEA (Sigma) and 6-AN (Aldrich) were treated once and left up to 72 hours. Cells treated with Polydatin and 5-FU (Sigma) combinations were replenished daily for up to 72 hours. Cells treated with DHEA and 5-FU combinations and 6-AN/5-FU combinations were treated once and left up to 72 hours. Thiazolyl blue tetrazolium bromide dye (MTT, Sigma-

Aldrich) at 5 mg/ml was added at each time point (final concentration 0.5 mg/ml). After 3 hours, the resultant intracellular formazan crystals were dissolved by adding 100  $\mu$ L of SDS-based solubilizing agent and left to incubate overnight. The absorbance (O.D.) was measured at 595 nm using the enzyme-linked immunosorbent assay (ELISA) microplate reader (Multiskan Ex).

#### **D. SRB Proliferation Assay**

The inhibitory effect of the following drugs was tested using the Sulforhodamine B (SRB) cell cytotoxicity assay kit (abcam 235935). It is a colorimetric assay based on total cellular protein content. HCT116, HCT116 p53<sup>-/-</sup>, and HCT116 5FU-R CRC cells were seeded in a 96-well plate at a density of 5,000 cells/well, left overnight, and treated the next day. HCT116 cells were treated either with a panel of different 6-AN concentrations or using 6-AN/5-FU combinations up to 72 hours. HCT116 5FU-R and HCT116 p53<sup>-/-</sup> were treated with 6-AN (10  $\mu$ M), 5-FU (5  $\mu$ M), or 6-AN (10  $\mu$ M) + 5-FU (5  $\mu$ M) up to 72 hours. The steps followed were utilized as per the manufacturer's protocol. Briefly, treated cells were treated using a fixation solution, washed, and incubated with the SRB salt to be stained by it. Next, cells were washed with a solubilization solution for bound SRB to dissolve. The plate was read at an absorbance of 595 nm using the ELISA Multiskan Ex microplate reader. This assay was used to confirm the results seen in the MTT assay results.

### **E. Compusyn**

To investigate the drug-drug pharmacodynamics, the software Compusyn was used to describe the interactions and to determine possible synergy. Cell viability of three different concentrations of each drug and their combinations obtained by MTT assay were fed into the software to evaluate drug/drug interactivity. According to this algorithm, a combination index (CI) higher than one indicates an antagonistic effect of the investigated drugs, a CI equal to one refers to an additive effect, while a CI lower than one indicates synergy.

### **F. Nitroblue Tetrazolium Reduction Assay**

HCT116 human CRC cells were seeded in triplicates in a 96-well plate at a density of 5,000 cells/well. Cells were incubated overnight and then treated with 6-AN (10  $\mu$ M), 5-FU (5  $\mu$ M), or 6-AN (10  $\mu$ M) + 5-FU (5  $\mu$ M). The levels of ROS produced were determined using the nitroblue tetrazolium (NBT) assay where NADPH reduced NBT salt into formazan that correlates with ROS levels. NBT (ARCOS) (1 mg/ml, 100  $\mu$ l) was added to control and treated wells and incubated for one hour. Then, cells were washed with methanol (100  $\mu$ l/well), and left to dry at room temperature. The formazan crystals were solubilized with potassium hydroxide (KOH) (2 M, 120  $\mu$ l) and dimethyl sulfoxide (DMSO) (140  $\mu$ l). The developed color was read at an absorbance of 630 nm using the enzyme-linked immunosorbent assay ELISA microplate reader MultiSkan Ex. The percentage of reduced NBT was calculated from the ratio of the absorbance obtained from

treated cells over control multiplied by 100. ROS levels were then determined by subtracting % NBT reduced from 100.

### **G. Cell Cycle Analysis**

HCT116 and HCT116 p53<sup>-/-</sup> cells were seeded in a 6-well plate at a density of 200,000 cells/well. Cells were incubated overnight and then treated the next day with 6-AN (10  $\mu$ M), 5-FU (5  $\mu$ M), or 6-AN (10  $\mu$ M) + 5-FU (5  $\mu$ M). Cell cycle analysis was performed using the propidium iodide (PI) assay. Cells were washed with 1x PBS, trypsinized, and harvested. Then cells were centrifugated at 1500 rotations per minute (rpm) for 5 minutes at 4°C. The supernatant was discarded, pellets were washed with ice-cold 1x PBS and centrifugated again at 1200 rpm for 5 minutes at 4°C. Cells were fixed with 80% ethanol and kept up to 10 days at -20°C. Next, fixed cells were incubated with 100  $\mu$ L RNase A (Roche Diagnostics) for 1 hour, resuspended in up to 500 ml 1x PBS, and then stained with 30  $\mu$ L PI (Sigma-Aldrich) then incubated for 10 minutes in the dark. 10,000 cells were collected and analyzed using FACScan flow cytometer (Becton Dickinson) and cell cycle distribution was verified using BD FACSDIVA software (Becton Dickinson).

### **H. G6PD Activity Assay**

The G6PD enzymatic activity was measured utilizing the G6PD colorimetric activity assay kit (abcam 102529). The assay is based on the oxidation of G6P to gluconate by G6PD present in the sample. HCT116, HCT116 p53<sup>-/-</sup>, and HCT116 5FU-R cells were

seeded at a density of 100,000 cells in a 6-well plate and incubated to settle overnight. These cells were then treated with 6-AN (10  $\mu$ M), 5-FU (5  $\mu$ M), or 6-AN (10  $\mu$ M) + 5-FU (5  $\mu$ M) for 48 hours. Total protein content was extracted using ice cold PBS by repetitive (10x) syringing and 5 cycles of freezing/thawing. Then, cells were centrifuged to collect proteins found in the supernatant, and quantified using the Bradford Protein Assay (Bio-Rad). A total of 10  $\mu$ g of protein was mixed with assay buffer, G6PD substrate, and G6PD developer according to the manufacturer's protocol. A positive and negative control ensured the assay was running correctly. Colorimetric measurement was read kinetically every 1 minute for 30 minutes at an O.D. of 450 nm at 37°C protected from light using the microplate Tristar multimode reader. The unit activity of the G6PD enzyme was defined as the amount of G6PD that will generate 1.0  $\mu$ mol of NADPH per minute at 37°C. The formula followed when calculating the activity was  $(B / (\Delta T \times V)) \times D$ . Where B = amount of NADPH present in the sample wells calculated from the standard curve obtained (nmol),  $\Delta T$  = linear phase reaction  $T_2 - T_1$  (minutes), V = original sample volume added into the reaction well (mL), and D = sample dilution factor.

### **I. Transketolase Assay**

The Transketolase (TKT) Human SimpleStep ELISA® kit (abcam 187398) quantitatively measures the amount of TKT present in human cells. Signals generated from the assay are measured colorimetrically and are proportional to the amount of TKT analyte present in the samples. HCT116 cells were seeded at a density of 1,500,000 cells in a 10 cm plate and incubated overnight. Cells were treated with 6-AN (10  $\mu$ M), 5-FU (5

$\mu\text{M}$ ), or 6-AN (10  $\mu\text{M}$ ) + 5-FU (5  $\mu\text{M}$ ) for up to 72 hours. Samples were solubilized and total protein lysates were extracted using cell extraction buffer supplied by the kit. Lysates were centrifugated, and quantified using the Bradford Protein Assay. 50  $\mu\text{L}$  of the sample (containing 100  $\mu\text{g}/\text{ml}$  protein) was topped with 50  $\mu\text{L}$  antibody cocktail into each well and incubated for 1 hour. Each well was washed and incubated with 3,3',5,5'-Tetramethylbenzidine (TMB) substrate. Color development was recorded kinetically for 15 minutes at 600 nm wavelength. Finally, the plate was read at an endpoint reading after adding a stop solution at an O.D. of 450 nm using the ELISA Multiskan Ex microplate reader.

#### **J. Glutathione Peroxidase Assay**

The Glutathione Peroxidase (GPx) assay kit (Cayman 703102) measures GPx activity indirectly by a coupled reaction with glutathione reductase (GR). Oxidized glutathione (GSSG) is produced by the reduction of hydroperoxide by GPx and is reduced back by GR and NADPH. The rate of decrease in absorbance is directly proportional to the activity of GPx in the sample. HCT116 cells were seeded at a density of 200,000 cells in a 6-well plate and incubated overnight. Cells were treated with 6-AN (10  $\mu\text{M}$ ), 5-FU (5  $\mu\text{M}$ ), or 6-AN (10  $\mu\text{M}$ ) + 5-FU (5  $\mu\text{M}$ ) for up to 48 hours. Whole cell lysates were prepared by a centrifugation step followed by two cycles of ultra-sonication in cold buffer supplied by the kit. The samples were centrifugated again and the supernatants were collected and quantified using the Bradford Protein Assay. The steps that followed were done according to the manufacture's protocol. Briefly, 50  $\mu\text{l}$  of the assay buffer, 50  $\mu\text{l}$  of the co-substrate,



50  $\mu$ l of NADPH, and 20  $\mu$ l of the protein sample (22  $\mu$ g) were mixed. The reaction took place upon the addition of 20  $\mu$ l cumene hydroperoxide and the absorbance was read kinetically every minute for 15 minutes at an O.D. of 340 nm using the ELISA Multiskan Ex microplate reader.

### **K. Western Blotting**

HCT116 cells were seeded at a density of 1,000,000 cells in a 10 cm plate and left to incubate overnight. Then cells were treated with 6-AN (10  $\mu$ M), 5-FU (5  $\mu$ M), or 6-AN (10  $\mu$ M) + 5-FU (5  $\mu$ M) for up to 72 hours. Total protein extracts (30  $\mu$ g) were obtained using Nonidet™ P 40-based lysis buffer (NP-40) and were quantified using the Bio-Rad Bradford Protein assay. Proteins were separated by SDS-PAGE (8-12%) under reducing conditions and transferred to nitrocellulose membranes. The latter were blocked for 1 hour at 37°C in 5% non-fat milk, then immunoblotted against G6PD (Abcam) (1:1000), TKT (Cell Signaling) (1:1000), B-cell lymphoma 2 (BCL-2) (Santa Cruz) (1:500), phosphorylated H2A histone family member X ( $\delta$ -H2AX) (Cell Signaling) (1:1000), p21 (Cell Signaling) (1:1000), BCL-2 associated X protein (BAX) (Cell Signaling) (1:500), Poly (ADP-ribose) polymerase (PARP) (Santa Cruz) (1:1000), and  $\beta$ -actin (Abcam) (1:1000), primary antibodies overnight. Then membranes were incubated for one hour against the corresponding secondary antibodies at different optimized dilutions. The immunoreactive bands were visualized by adding using the Western Blotting Luminol Reagent (Santa Cruz) and the Clarity™ enhanced chemiluminescence reagent (ECL, Bio-Rad), and imaged the Chemidoc™ MP Imaging System (Bio-Rad).

## **L. Statistical Analysis**

All the results represent the average of three independent experiments  $\pm$  standard error of the mean (SEM) unless stated otherwise. Result comparisons were analyzed by ANOVA analysis using GraphPrism. *P* values less than 0.05 were considered significant from the control. \*, \*\*, \*\*\* indicate *P* values less than 0.05, 0.01, and 0.001, respectively.

## CHAPTER IV

### RESULTS

#### A. G6PD Expression is Elevated in Colorectal Cancer Tissues

The expression of *G6PD* in human tissues was conducted through *in silico* analysis of *G6PD* mRNA expression in publicly available databases offering a wide collection of genetic expression profiles pertaining to colorectal tumors and normal counterparts (Figure 12). Data was filtered for colon and rectal tissues and was focused on *G6PD* expression in studies that had a *P* value < 0.05. As expected, colorectal pre-malignant (adenoma) and malignant (carcinoma and adenocarcinoma) tissues showed a higher *G6PD* mRNA level when compared to normal rectum or different colon sections in all the selected studies.

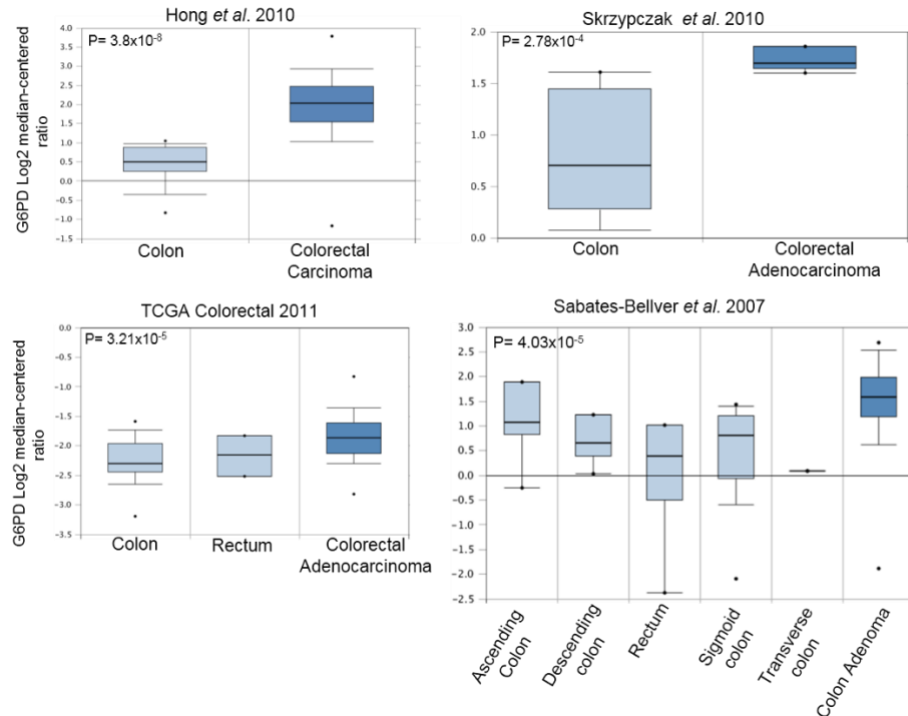


Figure 12. *G6PD* levels are elevated in colorectal cancer. Expression levels of *G6PD* mRNA were evaluated in publicly available datasets comprised of malignant and premalignant (adenoma) lesions of the colon and rectum along with normal colonic and rectal tissues. *P* values < 0.05 are considered statistically significant. Boxplots are obtained from oncomine.com.

## B. G6PD Inhibitors Suppress the Growth of HCT116 Colorectal Cancer Cells

To characterize the effect of G6PD inhibitors in CRC, HCT116 cells were treated with three different G6PD inhibitors (Polydatin, DHEA, and 6-AN) for up to three days (Figures 13-17).

### 1- Panel Treatment on HCT116

To investigate the effect of Polydatin, a specific G6PD inhibitor, in CRC, HCT116 cells were treated with different concentrations of Polydatin ranging between 12.5  $\mu\text{M}$  and 400  $\mu\text{M}$  and cell growth was assessed by MTT assay. Results showed a dose- and time-dependent inhibition of cell growth, with a significant reduction by 30 % in HCT116 cells growth observed at as low as 100  $\mu\text{M}$  on day 1 and by 20 % when using 25  $\mu\text{M}$  of Polydatin on days 2 and 3 after treatment when compared to control cells (Figure 13).

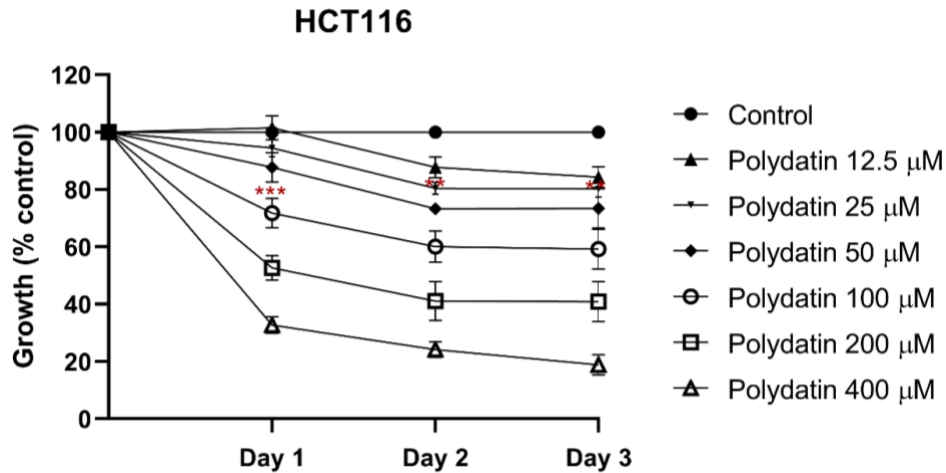


Figure 13. Polydatin treatment shows a concentration and time-dependent reduction of cell growth in HCT116 human colorectal cancer cells. Cells were treated with the indicated concentrations of Polydatin with daily replenishment for up to three days and cell growth was measured in triplicate wells using the MTT cell proliferation assay. Results are expressed as percentage of control and represent the average of at least three independent experiments  $\pm$  SEM. \*\* $P$  values  $< 0.01$  and \*\*\* $P$   $< 0.001$  are considered statistically significant.

## 2- DHEA Treatment on HCT116

The steroid DHEA is known to be an allosteric inhibitor of G6PD. Therefore, we determined its effect on HCT116 cellular growth. Cells were treated with a panel of DHEA concentrations ranging between 1  $\mu\text{M}$  and 20  $\mu\text{M}$  for up to 3 days (Figure 14) to study the DHEA effect of inhibiting the G6PD enzyme on these cells. Results presented that the use of 20  $\mu\text{M}$  DHEA was able to significantly inhibit 20% cell proliferation at day 1 and 5  $\mu\text{M}$  DHEA was able to significantly reduce cellular growth by 20% at days 2 and 3 of treatment (Figure 14). Whereby, DHEA concentrations lower than that had a minimal effect on growth inhibition when compared to untreated cells.

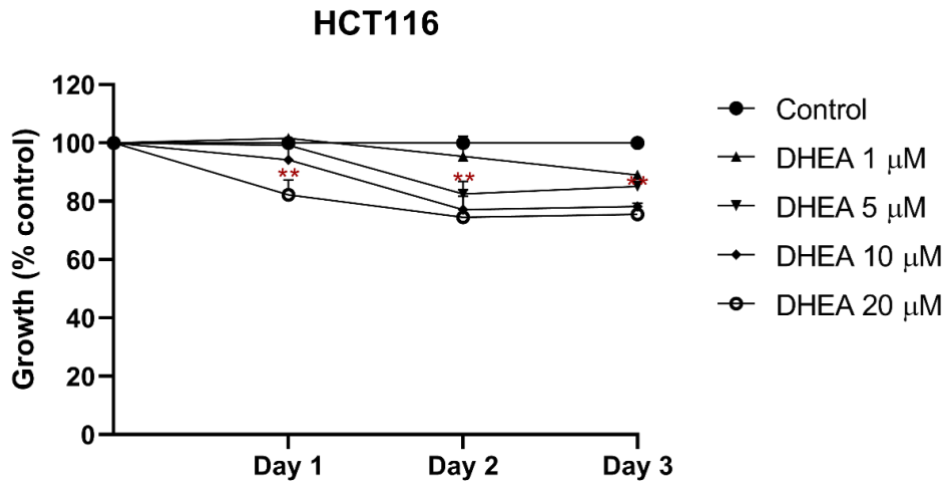


Figure 14. Effect of DHEA treatment on cell growth of HCT116 human colorectal cancer cells. Cells were treated with the indicated concentrations of DHEA for up to three days and cell growth was measured in triplicates using the MTT cell proliferation assay. Results are expressed as percentage control and represent the average of at least three independent experiments  $\pm$  SEM. **\*\****P* values < 0.01 are considered statistically significant

### 3- 6-aminonicotinamide Treatment on HCT116

Next, in order to study the effect of inhibiting both reducing enzymes of the oxidative phase of the PPP (G6PD and 6-PGD), the competitive G6PD inhibitor 6-AN was tested on CRC growth. HCT116 cells were treated with a panel of 6-AN concentrations ranging from 1.25  $\mu\text{M}$  to 40  $\mu\text{M}$  for up to 3 days (Figure 15). Cell proliferation was assessed by MTT, and results revealed that 6-AN treatment had a dose- and time-dependent effect on HCT116 cell growth inhibition, with a significant reduction in cell proliferation was recorded at as low as 1.25  $\mu\text{M}$  6-AN, where viability reached 90% at day 1 and 80% on day 2 and day 3 post-treatment.

Consequently, inhibiting both G6PD and 6-PGD enzymes showed an enhanced effect in limiting HCT116 cell proliferation in comparison to Polydatin and DHEA. Thus, when comparing the different G6PD inhibitors, 6-AN was found to have the most potent effect.

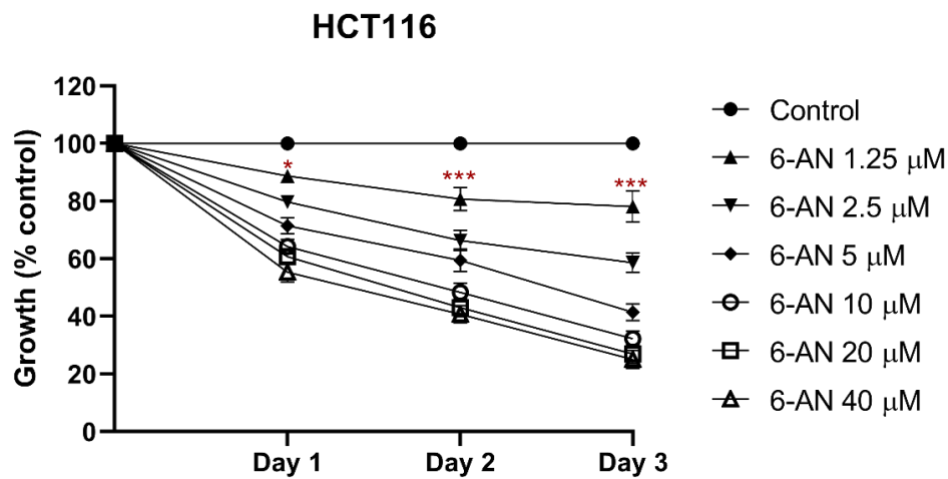


Figure 15. 6-AN treatment shows a concentration and time-dependent reduction of cell growth in HCT116 colorectal cancer cells. Cells were treated with the indicated concentrations of 6-AN for up to three days and cell growth was measured in triplicate wells using the MTT cell proliferation assay. Results are expressed as percentage of control and represent the average of at least three independent experiments  $\pm$  SEM. \* $P$  values  $< 0.05$  and \*\*\* $P < 0.001$  are considered statistically significant.

The colorimetric MTT assay measures cellular metabolic activity, therefore inhibiting G6PD might reduce NADPH-dependent cellular enzymes thus reflecting an incorrect number of viable cells. Therefore, we verified our cell growth results by the means of a different viability assay using SRB dye. The SRB assay is based on the binding of a bright pink dye to basic amino acids of viable cells under mildly acidic conditions. HCT116 cells treated with a panel of 6-AN concentrations (1.25  $\mu$ M – 40  $\mu$ M) for up to 3 days were assessed by SRB assay. Both MTT and SRB methods revealed similar growth inhibition trends with minimal discrepancies. However, SRB revealed higher drug effect towards cellular inhibition. This confirmed the previously obtained MTT results suggesting that 6-AN and MTT dye mechanism of action are independent (Figure 16).

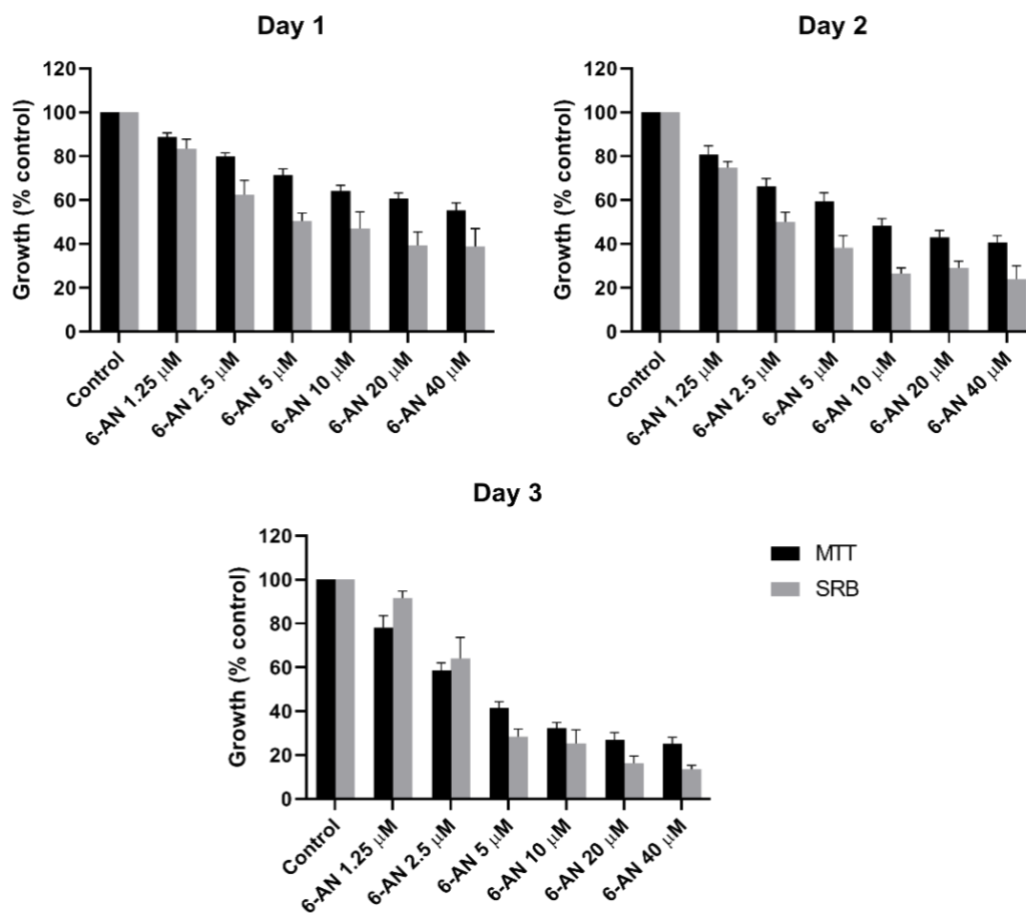


Figure 16. MTT and SRB assays indicate similar trends on the growth of 6-AN treated human colorectal cancer cells. Comparison of the effect of a panel of the indicated 6-AN concentrations on HCT116 cell growth using MTT and SRB assays in treated cells up to 3 days. Results are expressed as percentage of control and represent the average of at least three independent experiments  $\pm$  SEM.

To verify the stability of the 6-AN drug, an MTT assay was conducted to confirm whether 6-AN treatment needs to be replenished daily for up to three days. Two MTT assays were run in parallel where in one HCT116 cells were treated with a panel of 6-AN concentrations and replenished daily, and in the other assay HCT116 cells were treated one day after seeding only without replenishment. The presented results showed similar



growth inhibition rates. This suggests that 6-AN has an irreversible effect on HCT116 cell growth (Figure 17) and does not require daily replenishment.

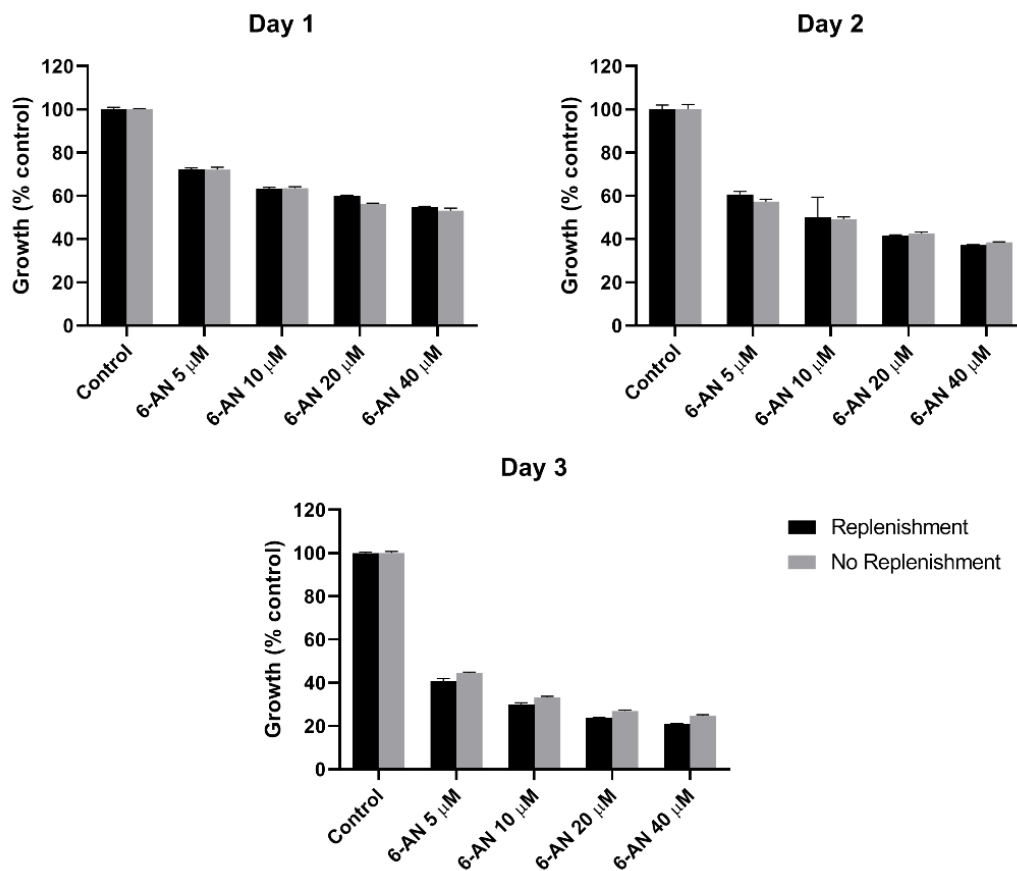


Figure 17. 6-AN treatment of colorectal cancer cells does not require daily replenishment. Comparison of the effect of a panel of the indicated 6-AN concentrations on HCT116 cells with and without daily replenishment for up to three days using the MTT assay. Results are expressed as percentage of control and represent the average of at least three independent experiments  $\pm$  SEM.

### **C. G6PD Inhibitors in Combination with 5-FU Further Suppress the Growth of Different Colorectal Cancer Cells**

To characterize the effect of G6PD inhibitors in CRC cells, HCT116 cells were treated with three different G6PD inhibitors (Polydatin, DHEA, and 6-AN) in combination with 5-FU for up to three days (Figures 18-21).

#### ***1- Polydatin and 5-FU Combination Treatment on HCT116***

To examine whether the effect of Polydatin in combination with chemotherapy would have any synergistic effect, HCT116 cells were treated simultaneously with Polydatin and 5-FU. The nine different treatment possibilities using Polydatin (25, 50, and 100  $\mu\text{M}$ ) and 5-FU (2.5, 5, and 10  $\mu\text{M}$ ) concentrations were assessed using MTT assay. The below graph is representative of all the possible combinations as none showed a synergistic effect (Figure 18). To further investigate the drug-drug interactions, the cell viability values obtained from these nine combinations were plotted using the Compusyn program. This software generated the CI of each treatment which described the interactions and determined the presence of synergy (Table 2). Treatments showed some antagonistic or additive effects of several combinations such as (Polydatin 10  $\mu\text{M}$  + 2.5  $\mu\text{M}$  5-FU at 24 hours), while other combinations (e.g. Polydatin 50  $\mu\text{M}$  + 2.5  $\mu\text{M}$  5-FU at 24 hours) showed a mathematical synergy that was insignificant biologically. The growth inhibition effect of the selected Polydatin/ 5-FU combination concentrations was scarcely different when compared to the treatment of any of the two single drug treatments, suggesting the low effectivity of this combination.

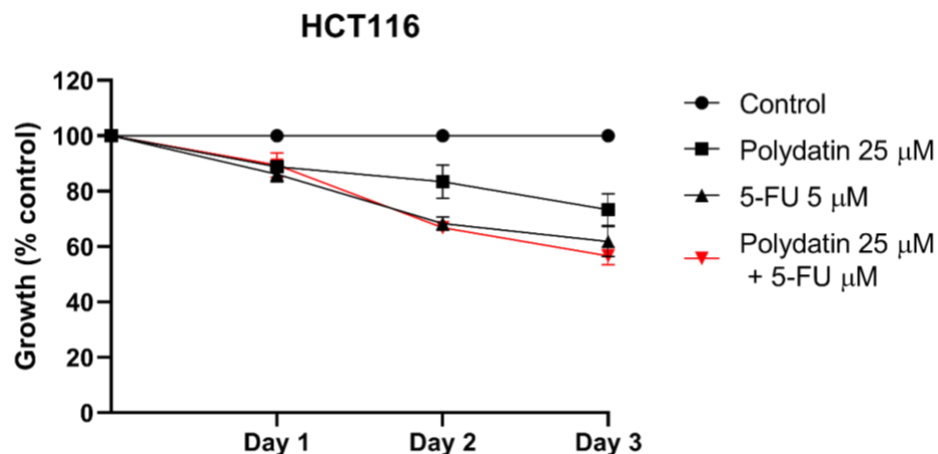


Figure 18. Effect of Polydatin and 5-FU combination treatment on HCT116 human colorectal cancer cells. Cells were treated with the indicated concentrations of Polydatin and/or 5-FU with daily replenishment for up to three days and cell growth was measured in triplicate wells using the MTT cell proliferation assay. Results are expressed as percentage of control and represent the average of at least three independent experiments  $\pm$  SEM.

24 hours			48 hours			72 hours		
Polydatin ( $\mu$ M)	5-FU ( $\mu$ M)	CI	Polydatin ( $\mu$ M)	5-FU ( $\mu$ M)	CI	Polydatin ( $\mu$ M)	5-FU ( $\mu$ M)	CI
10	2.5	3080	10	2.5	5.38	10	2.5	5.65
10	5	46.5	10	5	2.45	10	5	1.5
10	10	6.98	10	10	1.34	10	10	0.88
25	2.5	202	25	2.5	2.04	25	2.5	1.1
25	5	18.75	25	5	1.18	25	5	0.71
25	10	1.18	25	10	0.97	25	10	0.71
50	2.5	0.98	50	2.5	1.1	50	2.5	0.93
50	5	2.55	50	5	0.99	50	5	0.81
50	10	7.85	50	10	0.87	50	10	0.75

Table 2. Polydatin and 5-FU Compusyn synergy study. Compusyn report generation shows the effect of combination treatment on HCT116 colorectal cancer cells on the CI for up to 3 days. Red values indicate synergy. CI= 1 additive effect, CI<1 synergistic, CI>1 antagonistic.

## 2- DHEA and 5-FU Combination Treatment on HCT116

Similarly to Polydatin, the combination of DHEA and 5-FU was investigated to test the effect of the dual inhibition of the G6PD activity and DNA synthesis. Therefore, HCT116 cells were treated with a panel of DHEA (1, 10, and 50  $\mu\text{M}$ ) and 5-FU (2.5, 5, and 10  $\mu\text{M}$ ) combination treatments. Figure 19 shows a representative graph as none of the combination treatments revealed biologically significant synergy. Table 3 represents all the considered combinations and their corresponding CIs. In general, the DHEA concentrations had an additive effect when used in combination with 5-FU.

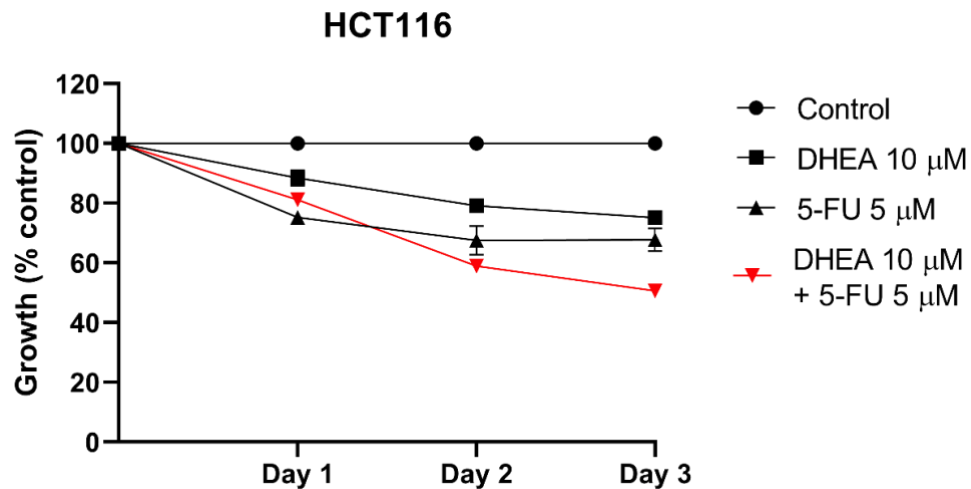


Figure 19. DHEA and 5-FU combination treatment on HCT116 human colorectal cancer cells. Cells were treated with the indicated concentrations of DHEA and/or 5-FU for up to three days and cell growth was measured in triplicate wells using the MTT cell proliferation assay. Results are expressed as percentage of control and represent the average of at least three independent experiments  $\pm$  SEM.

24 hours			48 hours			72 hours		
DHEA ( $\mu\text{M}$ )	5-FU ( $\mu\text{M}$ )	CI	DHEA ( $\mu\text{M}$ )	5-FU ( $\mu\text{M}$ )	CI	DHEA ( $\mu\text{M}$ )	5-FU ( $\mu\text{M}$ )	CI
1	2.5	2.12	1	2.5	3.13	1	2.5	2.89
1	5	1.66	1	5	1.65	1	5	1.25
1	10	1.84	1	10	1.3	1	10	1.27
10	2.5	1.56	10	2.5	0.96	10	2.5	1.22
10	5	1.72	10	5	0.7	10	5	0.71
10	10	2.03	10	10	0.75	10	10	0.73
50	2.5	1.15	50	2.5	1.17	50	2.5	0.73
50	5	1.73	50	5	1.34	50	5	0.77
50	10	2.32	50	10	1.46	50	10	0.93

Table 3. DHEA and 5-FU Compusyn synergy study. Compusyn report generation showed the effect of combination treatment on HCT116 colorectal cancer cells on the CI. Red values indicate synergy. CI= 1 additive effect, CI <1 synergistic, CI > 1 antagonistic

### 3- 6-AN and 5-FU Combination Treatment on HCT116 Cells

Next, to study the consequence of simultaneously inhibiting the main enzymes of the oxidative phase of the PPP, we studied the effect of the concurrent combination treatment of 6-AN on 5-FU had on CRC cells. Therefore, HCT116 cells were treated with the nine different concentrations generated from the panel of 6-AN (5, 10, and 20  $\mu\text{M}$ ) and 5-FU (2.5, 5, and 10  $\mu\text{M}$ ) combinations using the MTT assay (Figure 20). The below graphs represent all the executed possible combinations tested over three days, whereby all of the combinations except those with 2.5  $\mu\text{M}$  5-FU showed a greater inhibition than when each drug was used alone. Compusyn algorithm revealed that synergy was observed in most of the conducted combinations (Table 4). The highest biologically significant synergy (CI = 0.36) was detected at 24 hours when 10  $\mu\text{M}$  6-AN was combined to 5  $\mu\text{M}$  5-FU (Table 4). Based on these values, this combination concentration was selected and used in the further conducted studies.

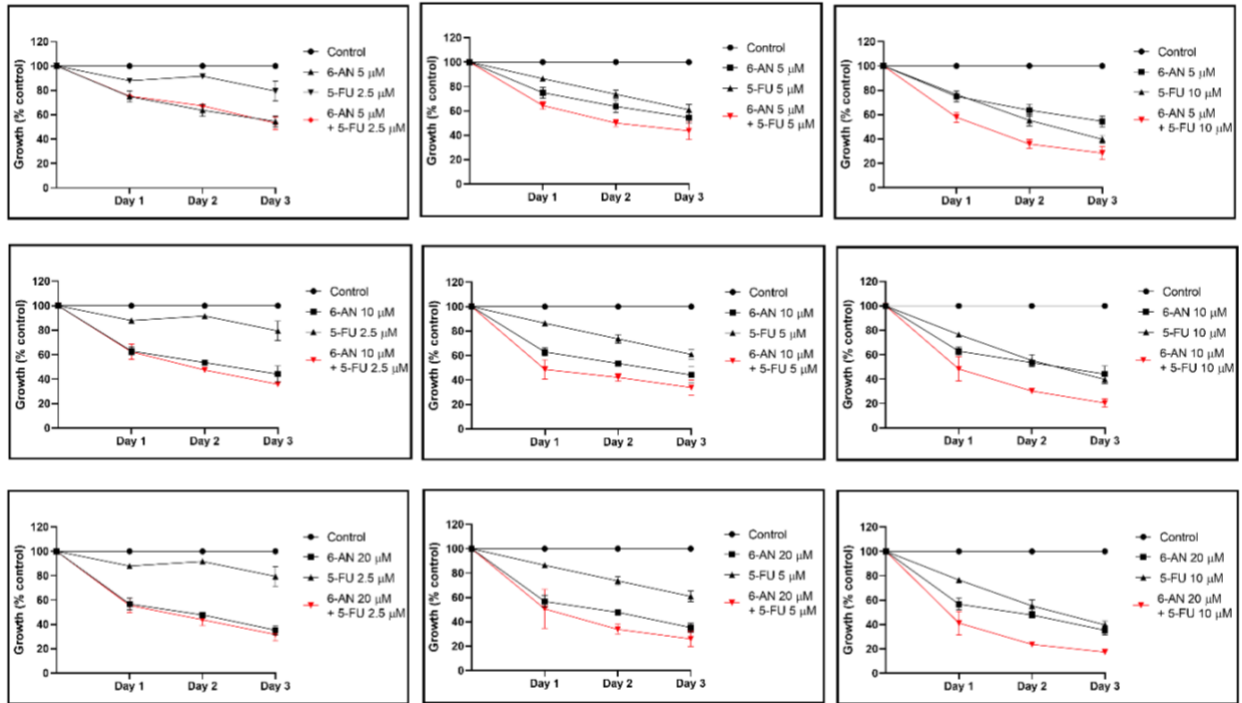


Figure 20. 6-AN and 5-FU combination treatments on HCT116 human colorectal cancer cells show synergistic interactions. Cells were treated with the indicated concentrations of 6-AN and/or 5-FU for up to three days and cell growth was measured in triplicate wells using the MTT cell proliferation assay. Results are expressed as percentage of control and represent the average of at least three independent experiments  $\pm$  SEM.

24 hours			48 hours			72 hours		
6-AN ( $\mu$ M)	5-FU ( $\mu$ M)	CI	6-AN ( $\mu$ M)	5-FU ( $\mu$ M)	CI	6-AN ( $\mu$ M)	5-FU ( $\mu$ M)	CI
5	2.5	1.27	5	2.5	1.77	5	2.5	1.27
5	5	0.59	5	5	0.78	5	5	1.05
5	10	0.47	5	10	0.74	5	10	0.79
10	2.5	0.83	10	2.5	0.7	10	2.5	0.76
10	5	0.36	10	5	0.7	10	5	0.88
10	10	0.38	10	10	0.65	10	10	0.59
20	2.5	1.06	20	2.5	0.95	20	2.5	1
20	5	0.78	20	5	0.59	20	5	0.79
20	10	0.42	20	10	0.56	20	10	0.58

Table 4. 6-AN and 5-FU Compusyn synergy study on HCT116-treated cells. Compusyn report generation for the effect of 6-AN and 5-FU combination treatment on HCT116 colorectal cancer cells on the combination index (CI). Red values indicate synergy. CI=1 additive effect, CI<1 synergistic, CI>1 antagonistic.

#### ***4- 6-AN and 5-FU Combination Treatment on HCT116, HCT116 p53<sup>-/-</sup>, and HCT116 5FU-R Cells***

An SRB viability assay was conducted on HCT116 cells using 6-AN (10  $\mu$ M) + 5-FU (5  $\mu$ M) to confirm results obtained through the MTT assay. The effect of this combination treatment was tested on HCT116 5FU-R and HCT116 p53<sup>-/-</sup> cells (Figure 21) since many patients develop resistance to 5-FU and *p53* gene is deregulated in around 50% of cancers. The data suggested that inhibiting G6PD and 6-PGD was able to sensitize 5-FU resistant cells as well as p53<sup>-/-</sup> cells to 5-FU.

6-AN enhanced the 5-FU effect in HCT116 5FU-R cells whereby at day 2, 5  $\mu$ M 5-FU induced 30 % cell growth inhibition while 60% was measured when 10  $\mu$ M 6-AN was combined to 5  $\mu$ M 5-FU (Figure 21). The combination of 6-AN (10  $\mu$ M) + 5-FU (5  $\mu$ M) on HCT116 p53<sup>-/-</sup> cells reported the lowest growth inhibition percentage (40% at 48 hours) while enhancing the effect of both drugs administrated alone (Figure 21).

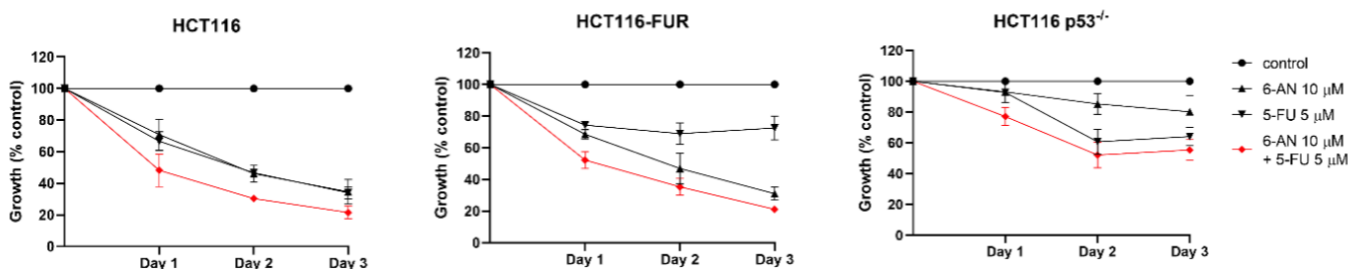


Figure 21. Comparison of the effect of 6-AN and 5-FU single and combination treatments on the growth of HCT116, HCT116-FUR, and HCT116 p53<sup>-/-</sup> human colorectal cancer cell lines. Cells were treated with the indicated concentrations of 6-AN/5-FU for up to three days and cell growth was measured in triplicate wells using the SRB cell proliferation assay. Results are expressed as percentage of control and represent the average of three independent experiments  $\pm$  SEM.

**D- 6-AN and/or 5-FU Treatment Did Not Modify G6PD nor TKT Protein Levels but Decreased G6PD Activity**

To support the fact that the effect of cell proliferation arrest of 6-AN was indeed through the inhibition of G6PD by 6-AN, G6PD activity and protein levels were measured. HCT116 cells were treated with 6-AN (10  $\mu$ M), 5-FU (5  $\mu$ M), or 6-AN (10  $\mu$ M) + 5-FU (5  $\mu$ M) for up to three days and cellular pellets were collected. Total SDS protein lysates were obtained from the different conditions and subjected to immunoblotting against G6PD. Results demonstrated that 6-AN did not modify G6PD protein levels when compared to untreated samples (Figure 22 A). These western blot results were only conducted once and need to be repeated at least twice for significance studies. Similarly, 5-FU and the combination treatment of 6-AN and 5-FU did not show any decrease in G6PD protein levels relative to actin. However, when evaluating activity through the G6PD enzymatic activity, it showed that 6-AN and the combination treatment did reduce G6PD activity in HCT116, HCT116 5FU-R, and in HCT116 p53<sup>-/-</sup> cells at 48 hours post-treatment (Figure 22 B), although not significantly.



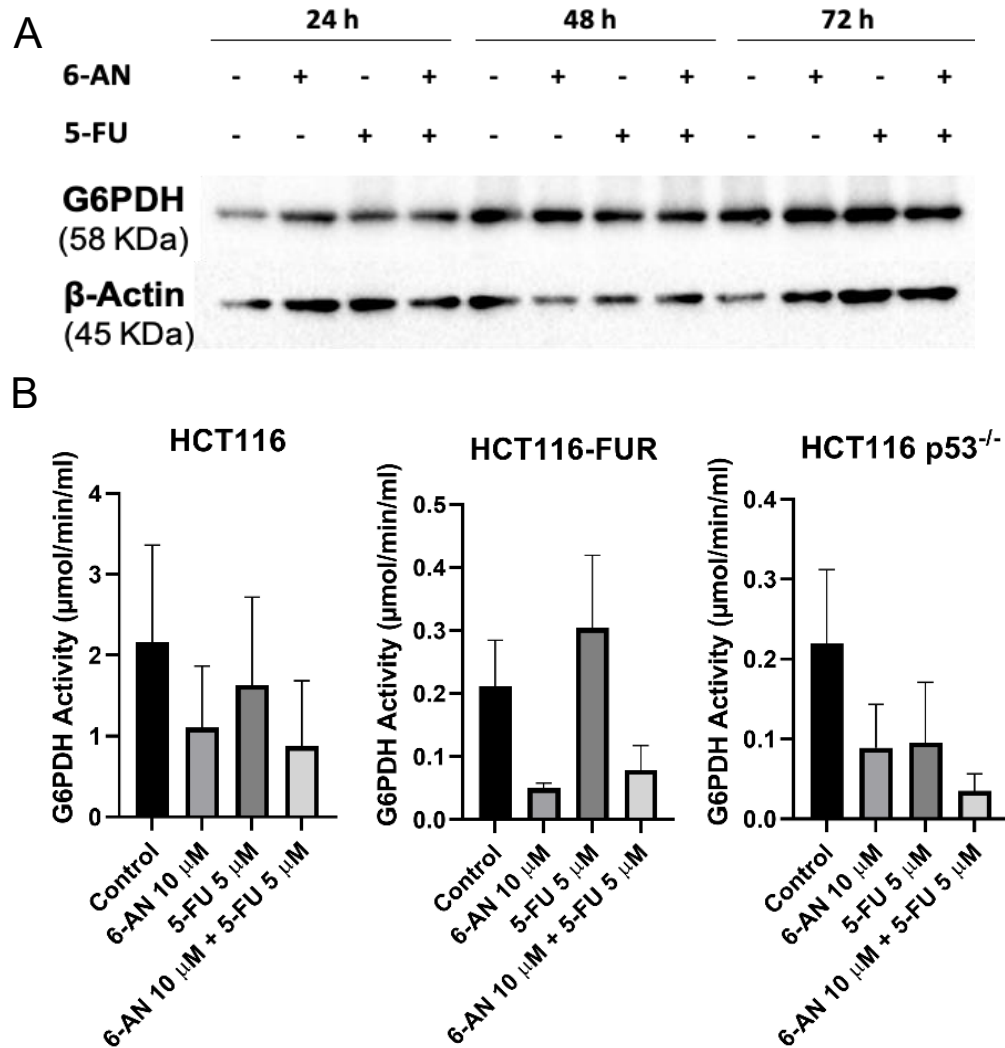


Figure 22. G6PD levels and activity upon 6-AN and/or 5-FU single and combination treatments of human colorectal cells. (A) HCT116 cells were treated with 6-AN (10  $\mu$ M) and/or 5-FU (5  $\mu$ M) for up to three days. Total SDS protein lysates (30  $\mu$ g) were immunoblotted against G6PD antibody.  $\beta$ -Actin was used as loading control. (B) G6PD activity was measured in human HCT116, HCT116 5FU-R, and HCT116 p53<sup>-/-</sup> colorectal cancer cells. Lysates (10  $\mu$ g) of cells treated with with 6-AN (10  $\mu$ M) and/or 5-FU (5  $\mu$ M) for 48 hours were collected. G6PD activity was measured according to manufacturer's recommendations. Results represent the average of three independent experiments  $\pm$  SEM.

Since G6PD is the rate limiting enzyme of the oxidative phase of the PPP, investigations were made to assess whether 6-AN had any implications on one of the major enzyme of the non-oxidative phase, TKT. Therefore, HCT116 cells were treated with 6-AN (10  $\mu$ M), 5-FU (5  $\mu$ M), or 6-AN (10  $\mu$ M) + 5-FU (5  $\mu$ M) for up to three days and cellular pellets were collected. TKT protein levels were measured (n=1) by immunoblotting (Figure 23 A) and were confirmed by the mean of a commercially available ELISA kit (Figure 23 B) (n=1, samples run in duplicates). Both methods showed that none of the treatments (6-AN and/or 5-FU) significantly modified TKT protein levels (Figure 23).

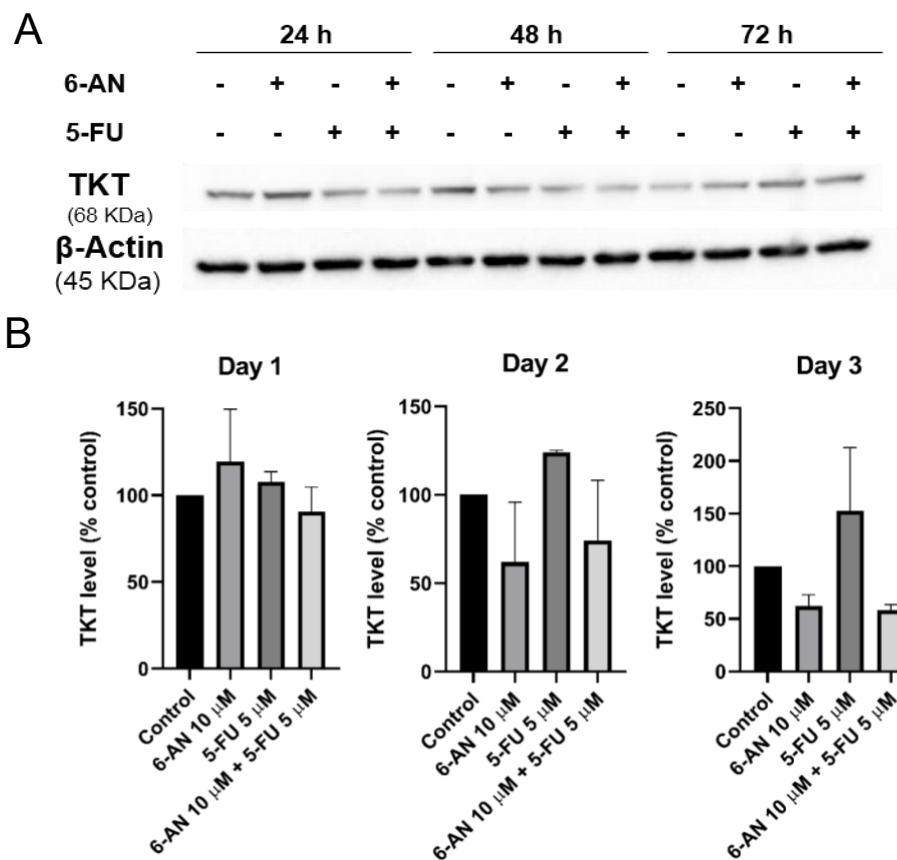


Figure 23. Transketolase levels are unaltered upon 6-AN and/or 5-FU single and combination treatment of human colorectal cells. (A) Cells were treated with the indicated concentrations for up to three days. Total SDS protein lysates (30  $\mu$ g) were immunoblotted against TKT antibody.  $\beta$ -Actin was used as loading control. (B) HCT116 cells were treated with with 6-AN (10  $\mu$ M) and/or 5-FU (5  $\mu$ M) for up to three days. Total cell lysate (100  $\mu$ g/ml) of the different conditions were collected and TKT levels were measured. Results represent the average of two measurements ( $\pm$  SD).

## **E- 6-AN and/or 5-FU Treatments Altered the Cell Cycle and Increased HCT116**

### **Cell Death**

Since 6-AN hinders cell proliferation through binding to G6PD and 5-FU arrests nucleotide biosynthesis, we aimed to explore the impact of 6-AN and 5-FU single or the combination treatments had on the progression of the cell cycle of HCT116 cells. Cell cycle analysis was conducted based on DNA content distribution stained with PI (Figure 24). The distribution of control cells in the sub-G1 phase was less than 5% at days 1 and 2 and 10% at day 3, thus indicating a minimum amount of cell death in control cells (Figure 24 A). Treatment of HCT116 cells with 5-FU (5  $\mu$ M) or 6-AN (10  $\mu$ M) + 5-FU (5  $\mu$ M) resulted in a significant increase in the sub-G1 region arrest by 15% and 10%, respectively at day 2. (Figure 24 A). Furthermore, when compared to the control, 6-AN (10  $\mu$ M), 5-FU (5  $\mu$ M), and the combination treatments of 6-AN (10  $\mu$ M) + 5-FU (5  $\mu$ M) significantly increased the S-phase arrest at day 1 by 21%, 77%, and 32%, respectively (Figure 24 B).

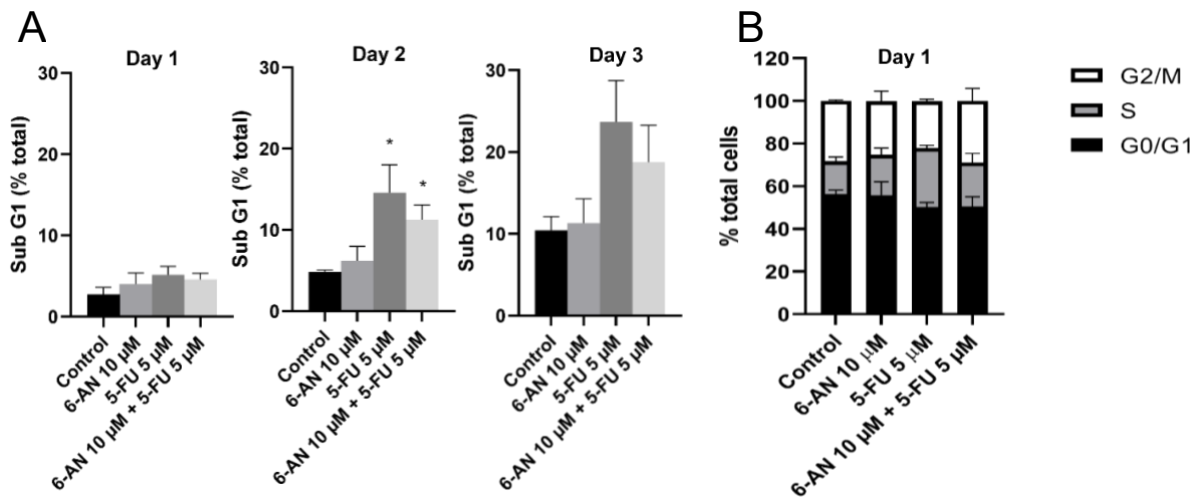


Figure 24. Cell cycle distribution of 6-AN and/or 5-FU treated HCT116 colorectal cancer cells. HCT116 cells were treated with 6-AN (10  $\mu$ M), 5-FU (5  $\mu$ M), or their combination up to three days and stained with propidium iodide (50 mg/ml). (A) Treatment induced an accumulation of cells in sub-G1 phase. (B) Cell cycle distribution of HCT116 cells treated with 6-AN (10  $\mu$ M) and/or 5-FU (5  $\mu$ M) for one day. The sum of G0/G1, S, and G2/M phases is a percentage of nonapoptotic cells. Percentage cells in the G0/G1 phase are calculated as 100 - (S+G2/M). Results represent three independent experiments ( $\pm$  SEM). (B) \**P* values < 0.05 are considered statistically significant.

To further investigate the mechanism of action of 6-AN (10  $\mu$ M), 5-FU (5  $\mu$ M), or 6-AN (10  $\mu$ M) + 5-FU (5  $\mu$ M) treatments in altering the cell cycle of HCT116 cells, samples were immunoblotted (n=1) with different cell cycle regulators and cell death proteins of interest (Figure 25). PARP cleavage was examined to explore the mechanism of cell death upon treatment since HCT116 cells presented a cell accumulation in the sub-G1 phase (Figure 24 A). However, PARP did not show significant cleavage, suggesting that apoptosis is not the mechanism of cell death. 5-FU (5  $\mu$ M) and 6-AN (10  $\mu$ M) + 5-FU (5  $\mu$ M) treatments substantially increased  $\gamma$ -H2AX levels indicating DNA damage. Furthermore, the S-phase arrest observed in flow cytometry (Figure 24 B) is concordant

with the increase in p21, a cyclin-dependent kinase inhibitor. Experiments should be repeated independently to calculate densitometry analysis on BAX:BCI2 ratio.

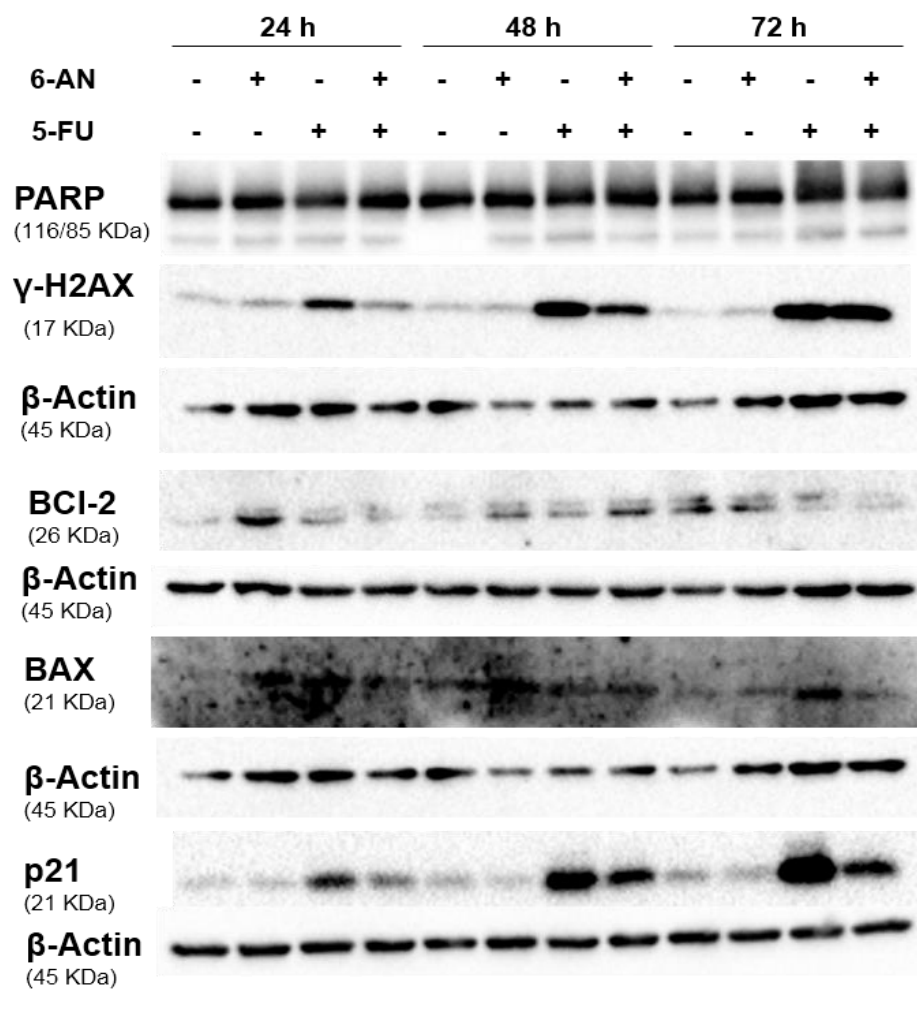


Figure 25. Mechanism of action of 6-AN and/or 5-FU treated HCT116 colorectal cancer cells. HCT116 cells were treated with 10  $\mu$ M 6-AN, 5  $\mu$ M 5-FU, or their combination up to three days. (B) Total SDS protein lysates (30  $\mu$ g) were immunoblotted against PARP,  $\gamma$ -H2AX, BCI-2, BAX, and p21 antibodies.  $\beta$ -Actin was used as loading control.

## **F- 6-AN and/or 5-FU Treatment Altered the Cell Cycle and Increased HCT116**

### **p53<sup>-/-</sup> Cell Death**

Next, to measure the effect on the cell cycle regulation of HCT116 p53<sup>-/-</sup> in response to 6-AN and/or 5-FU combination treatments, flow cytometry analysis was performed (Figure 26). The distribution of control cells in the sub-G1 phase was less than 5% at all three time points indicating a minimum amount of cell death in control samples (Figure 26 A). Treatment of 5-FU (5  $\mu$ M) and 6-AN (10  $\mu$ M) + 5-FU (5  $\mu$ M) increased cell death significantly at day 2 and 3, respectively reaching 29% and 23% increase at day 2, and 31% and 28% at day 3 (Figure 26 A). Moreover, the 5-FU (5  $\mu$ M) and 6-AN (10  $\mu$ M) + 5-FU (5  $\mu$ M) treatments at day 1 increased the G0/G1 phase accumulation of 30% and 40%, respectively. 6-AN single treatment had no substantial effect on the HCT116 p53<sup>-/-</sup> cell cycle (Figure 26 B).

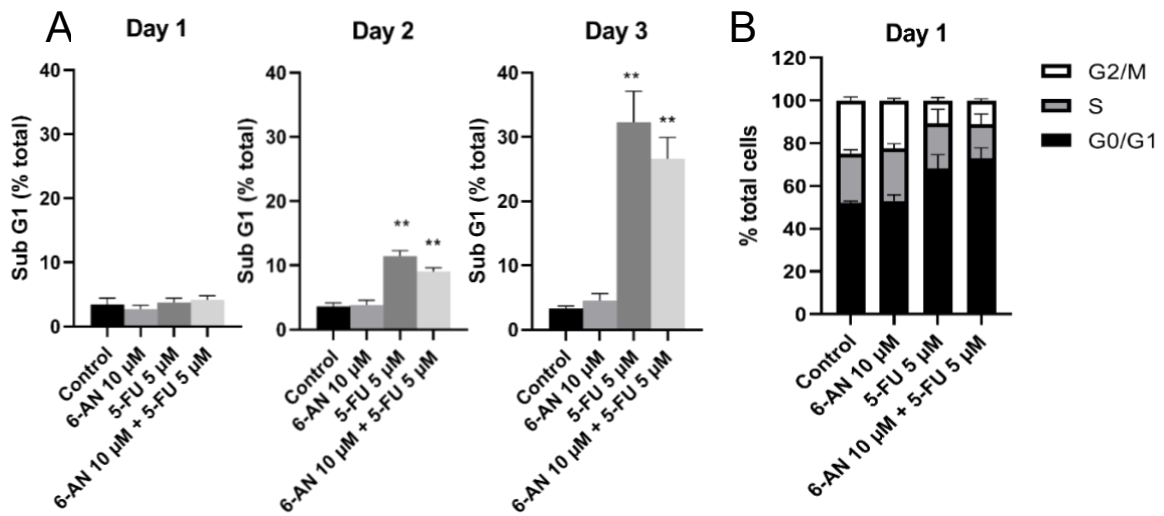


Figure 26. Cell cycle distribution of 6-AN and/or 5-FU treated p53<sup>-/-</sup> colorectal cancer cells. HCT116 p53<sup>-/-</sup> cells were treated with 6-AN (10  $\mu$ M) and/or 5-FU (5  $\mu$ M) for up to three days and stained with propidium iodide (50 mg/ml). (A) The combination treatment induced significant accumulation of cells in sub-G1 phase. (B) Cell cycle distribution of HCT116 p53<sup>-/-</sup> cells treated with 6-AN (10  $\mu$ M) and/or 5-FU (5  $\mu$ M) for 1 day. The sum of G0/G1, S, and G2/M phases is a percentage of nonapoptotic cells. Percentage cells in the G0/G1 phase are calculated as 100 - (S+G2/M). Results represent three independent experiments ( $\pm$  SEM). \*\**P* values < 0.01 are considered statistically significant.

### G- 6-AN and 5-FU Combination Induced Reactive Oxygen Species Generation in HCT116 Cells

Reduction of NADPH levels due to PPP inhibition favors an increase in oxidative stress. Therefore, ROS production was assessed in HCT116 treated with 6-AN and/or 5-FU for up to 3 days using NBT reduction assay (Figure 27, n=2). No ROS production was detected at day 1 (data not shown). HCT116 cells treated with the combination of 6-AN (10  $\mu$ M) + 5-FU (5  $\mu$ M) increased ROS production by 20 % compared to cells treated with 6-AN (10  $\mu$ M) alone, at day 2. Furthermore, 6-AN and/or 5-FU treated cells at day 3 revealed



an elevated ROS production compared to untreated counterparts (Figure 27). This experiment should be repeated one more time to evaluate statistical significance.

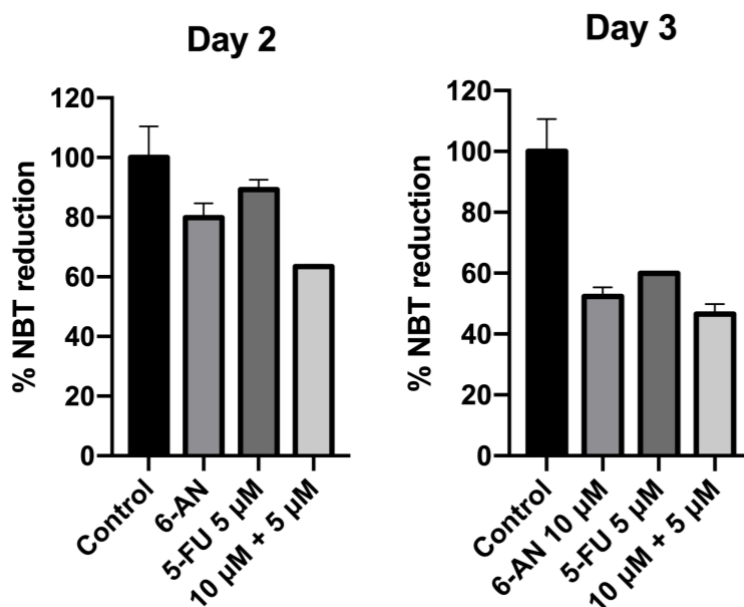


Figure 27. Effect of 6-AN and/or 5-FU on NBT reduction (inversely correlated to ROS generation) in HCT116 human colorectal cancer cells using NBT assay. Treatment with 6-AN and/or 5-FU increases ROS levels. HCT116 human colorectal cells were treated with the indicated concentrations of 6-AN and/or 5-FU for up to three days. ROS levels were determined in triplicate measurements using the NBT reduction assay. ROS levels were calculated by subtracting % NBT reduced from 100. Results represent the average of two independent experiments ( $\pm$  SD).

#### H- 6-AN and 5-FU Combination Increased Glutathione Peroxidase (GPx) Activity

Glutathione is the main intracellular thiol that serves a protective role in cellular defense against oxidative stress. G6PD activity in the normal and the different tumor cell lines affect the levels of NADPH, and subsequently the reduced glutathione (GSH) levels. GPx converts GSH into oxidized glutathione (GSSG) and thus reflects ROS detoxification. Whole cell lysates of HCT116 cells treated with 6-AN (10  $\mu$ M) and/or 5-FU (5  $\mu$ M) up to 48 hours were used to assess GPx activity (Figure 28, n=1). No change in activity was

observed at 6 and 24 hours. However, the combination treatment of 6-AN (10  $\mu$ M) + 5-FU (5  $\mu$ M) increased GPx activity by 50% compared to control and single drug treatments (Figure 28). This experiment was conducted once and, therefore, needs to be repeated at least twice for statistical and biological significance.

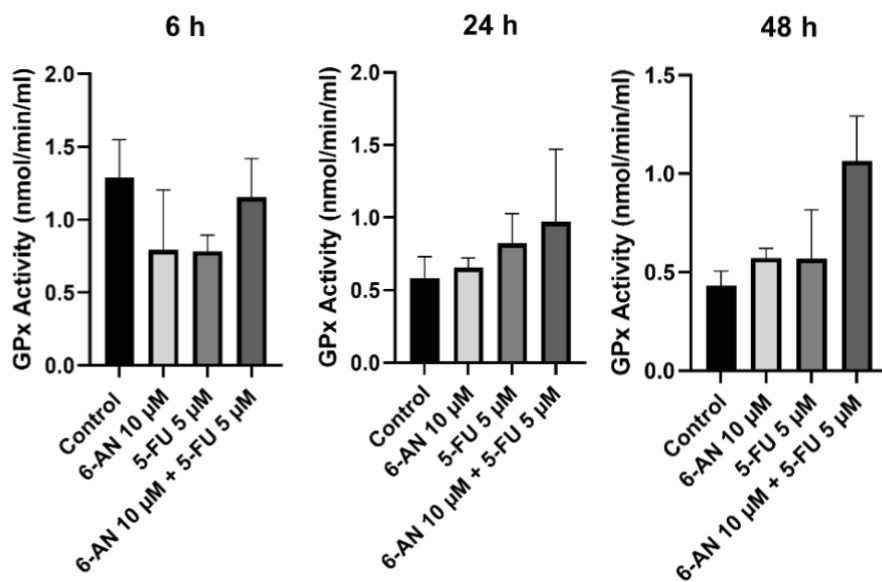


Figure 28. Effect of 6-AN and/or 5-FU on GPx activity in HCT116 human colorectal cancer cells. HCT116 cells treated with the indicated concentrations of 6-AN and/or 5-FU for up to 48 hours. GPx activity was determined in duplicate measurements. Results represent the average of two measurements ( $\pm$  SD).

## CHAPTER V

### DISCUSSION

Colorectal cancer is the third most common cancer and the second cause of cancer-related death worldwide (WHO, 2018). Numerous areas of cancer research have been exhaustively and extensively studied, therefore targeting cancer progression from a metabolic perspective might offer unique therapeutic opportunities. Energy metabolism is reprogrammed in many tumors, and these alterations confer a growth advantage in cancer (Patra et al., 2014). Cancer cells develop a network of interconnected signaling events that lead to initiation and progression in which cellular metabolism, including the PPP, is an indispensable part of it (Hanahan et al., 2011). The PPP is an essential pathway for glucose metabolism that is diverted from glycolysis. It offers anabolic properties and supplies the cells with NADPH that has reducing capabilities and scavenges ROS. This pathway also provides the cell with R5P, a precursor for DNA and RNA nucleotide biosynthesis (Patra et al., 2014).

This research focuses on the therapeutic targeting of the PPP in CRC. We aimed here to use PPP inhibitors and not upstream inhibitors of the general glucose metabolic pathway. Targeting the hexokinase enzyme or halting glycolysis (Tsouko et al., 2014), for example, would lead to off-target alterations and impedes the performance of *in vivo* studies. Inhibiting the main and well-regulated enzymes of the PPP, including G6PD and 6-PGD, may offer a new therapeutic window to approach cancer treatment. Using *in silico* analysis, we showed that the basal *G6PD* mRNA level are overexpressed in CRC tissue compared to

healthy counterparts (Figure 12). This led us to investigate whether therapeutically targeting *G6PD* would hinder its overactivation.

6-AN (Herken, 1968) and DHEA (Klinge et al., 2018) are well-known inhibitors of G6PD, however whether the activity of DHEA inhibition is non-competitive or uncompetitive on G6PD remains inconclusive. Polydatin has been recently characterized as a non-competitive inhibitor of G6PD (Mele et al., 2018). Using a panel of different concentrations of these drugs we investigated their effect on HCT116 CRC growth. 6-AN showed the most favorable response in cell viability reduction (Figure 17) when compared to DHEA (Figure 15) or to Polydatin (Figure 13) responses. Testing the effect of 6-AN on the normal-like colon cell line (NCM460D) were the least affected cell line when compared to HCT116 cells with different p53 and p21 statuses (Al Saleh et al., 2018). This makes the usage of 6-AN favorable as a chemotherapeutic drug because of its ability to spare normal tissue.

We hypothesize that 6-AN has shown the highest inhibitory response due to the fact that it inhibits both dehydrogenase enzymes of the PPP, G6PD and 6-PGD (Budihardjo et al., 1998), which makes it a more potent inhibitor. The plant-derived Polydatin molecule is a naturally occurring compound, and thus high administered dosages may seem to have a more appealing clinical potential and might offer lower side effects (Rajesh et al., 2015).

Using the Compusyn software, we were able to generate 81 different CIs for three different drugs, at three different time points, using three different concentrations, each in combination with 5-FU. Interestingly, 6-AN combined with 5-FU had the most favorable response in lowering HCT116 cell viability (Figure 20). Particularly when combining 10  $\mu$ M of 6-AN with 5  $\mu$ M of 5-FU, we obtained the lowest CI observed. The rationale behind

combining these drugs with 5-FU is to deplete cellular energy sources and to inhibit DNA synthesis and repair (Almugadam et al., 2018).

Owing to the fact that 5-FU is the standard reference chemotherapeutic drug in CRC and many patients develop drug resistance (Sara et al., 2018), we aimed to tackle 5-FU resistance in HCT116 cells. Therefore, in an effort to overcome this resistance, we combined 6-AN with 5-FU to explore whether it would sensitize HCT116 5FU-R cells, HCT116 cells resistant to high doses of 5-FU. Our results suggest that 6-AN combined to 5-FU sensitizes HCT116 5FU-R cells as a greater growth inhibition effect was observed when compared to 6-AN or 5-FU treatments alone (Figure 21). Lastly, this combination also showed a more significant growth inhibition when tested on HCT116 *p53*<sup>-/-</sup> cells, an aggressive cell line and where *p53* is deregulated in 50% of human CRC tumors.

5-FU has been shown to lower G6PD activity, increase nitric oxide (NO) production, and elevate ROS levels (Focaccetti et al., 2015). NO induces cell cycle arrest, mitochondrial depolarization, and apoptosis (Jahani et al., 2017). This is a proposed mechanism of the synergy observed in our study whereby 6-AN and 5-FU both inhibit PPP-related enzymes and alterate free radicals levels.

Moreover, MTT replenishment assay indicated that neither 6-AN (Figure 18) nor DHEA (data not shown) needed daily replenishment, whereas Polydatin must be replenished daily (data not shown). Since the MTT assay measures cellular viability based on the reducing power of mitochondria, it was evident that 6-AN did not interfere with this pathway after performing the SRB assay in parallel, which assesses cellular viability considering the total protein content of the cell (Figure 19).

Mechanistically, we showed that 6-AN, 5-FU, or 6-AN/5-FU combination treatments did not alter G6PD nor TKT protein expression levels suggesting the drugs may work independently from mRNA transcription or translation (Figures 22 and 23). However, treatments were able to reduce the activity of G6PD in all tested cell lines. Interestingly, the combination treatment suggests a potent synergistic inhibition of G6PD activity in HCT116 p53<sup>-/-</sup>. This can be validated further through *in vivo* models whereby the inhibition of this enzyme may have many promising implications in treatment, particularly in the setting of 5-FU resistance or p53 mutation. The results obtained, however, did not reach significance and must be repeated with lower variability and where higher drug concentrations can be used. TKT levels were measured using western blotting and validated through an ELISA assay. Both experiments showed the amount of TKT protein to remain unaltered by 6-AN, 5-FU, or 6-AN/5-FU combination treatment. Further experiments are needed to determine if this treatment alters the enzymatic activity of TKT. Previously obtained data in our lab (Al Saleh et al., 2018) showed that HCT116 p53<sup>-/-</sup> had a lower G6PD activity than the HCT116 cells wild type for p53, however, the present results showed otherwise. This discrepancy might be due to the fact that different protocols were used and further optimization is needed to be performed at the level of each cell line.

Cell cycle deregulation is a common feature in human tumors (Malumbres et al., 2009). To gain insight into the mechanism of cell death, we analyzed the cell cycle of HCT116 cells upon combination treatment. Results showed that there was an increase in cell death two days post-treatment. These cells are presumably apoptotic as indicated by the less than 2n DNA content which infers DNA fragmentation. However, further experiments such as the TUNEL assay are needed to confirm the mode of death observed. Moreover, 5-

FU treatment increased the S-phase arrest of HCT116 cells (Figure 24). Importantly, cells left in culture for longer time points may provide further understanding of the mechanism of cell death in these cell lines and whether the combination treatment induces senescence such as when cells were treated with 50  $\mu$ M of 6-AN (Al Saleh et al., 2018).

Immunoblotting showed that the death observed initially up to three days did not induce PARP cleavage, suggesting it to be a caspase 3-independent death. Of note, 6-AN was shown to be a weak inhibitor of PARP (Sims et al., 1982) (Figure 25). Longer cell death time points and other modes of non-apoptotic cell death should be investigated. 5-FU and 6-AN/5-FU combination treatment substantially increased levels of  $\delta$ -H2AX, which is indicative of DNA damage. The BAX protein has a critical role in tumor response to chemotherapy that may influence cell metabolism, and the BAX/BCL-2 serves as a marker to determine cell susceptibility to apoptosis (Salakou et al., 2007). However, immunoblotting against these proteins must be independently repeated for more definite results with densitometry analysis. p21 is a cyclin-dependent kinase (CDK) and CDK/cylin complex inhibitor and is known to be upregulated in senescent cells (Georgakilas et al., 2017). The upregulation of p21 protein expression on day one upon 5-FU treatment is concomitant with the S-phase arrest seen in HCT116 cells. Altogether, the 6-AN/5-FU combination treatment alters the cell cycle, and preliminary evidence suggests that treatment induces caspase3-independent death. Moreover, 5-FU and 6-AN/5-FU combination treatments induced a G0/G1 phase arrest on day one and increased cell death on day two and day three in HCT116 p53<sup>-/-</sup> cells (Figure 26). Western blotting must be conducted to investigate the mechanism of action leading to this increase.

ROS generation plays a major role in cancer signaling and progression. It is an essential part of the cell life cycle, and its overproduction can have detrimental effects on cell viability, as it can damage the DNA and inhibit proliferation (McConnell et al., 2018). Here, we show that the inhibition of the two main dehydrogenase enzymes of the oxidative phase of the PPP leads to an accumulation of ROS production (Figure 27). These enzymes are known to aid in the detoxification and scavenging of ROS and other free radicals. Interestingly, the percentage of ROS generation increased upon treatment with 6-AN, which is in harmony with our hypothesis stating that inhibiting G6PD would halt tumor progression. Moreover, the combination treatment of 6-AN (10  $\mu$ M) + 5-FU (5  $\mu$ M) further increased ROS production. This is concordant with the high inhibitory synergistic effect seen through the Compusyn algorithm.

Glutathione is the main intracellular thiol that serves a protective role in cellular defense against oxidative stress. Glutathione peroxidase, GPx, catalyzes the reduction of hydroperoxides, including H<sub>2</sub>O<sub>2</sub>, into water while using reduced glutathione, GSH (Figure 7). GPx functions to protect the cell from oxidative damage and participates in the electronic reduction of the peroxide substrate (Dalvi et al., 2012). In the assay we conducted, the rate of decrease in absorbance observed was directly proportional to the GPx activity in the sample. The increase in GPx activity seen in HCT116 cells upon treatment (Figure 28) might be due to the increased ROS production (Figure 27), thereby inducing a negative feedback mechanism to lower free radical levels. It is possible that the increased levels of ROS led to a regulation in GPx activity to detoxify ROS.

In conclusion, our findings demonstrate that combining the G6PD inhibitor 6-AN to 5-FU may decrease resistance and further sensitize CRC cells to chemotherapy



independently of their *p53* and 5-FU resistance status. This study provides further understanding into areas of current knowledge on CRC and cancer metabolism while recognizing that the insights presented are only fragments of the total picture.

#### Limitations of the Study

Although this study provides novel information on the combination treatment of 6-AN and 5-FU in the CRC setting, it does not go without limitations and restrictions. Some experiments must be replicated independently to validate our results. Other experiments need to be repeated to achieve lower variability and ultimately reach statistical significance.

Moreover, we are aware of the fact that *in vitro* results do not necessarily reflect *in vivo* or physiological settings. Therefore, the translation of this work into an animal model is crucial for moving forward with these findings. In this study, we focused on the PPP and a few associated proteins. We acknowledge that the PPP is largely interconnected with the complex cancer metabolic network and interplays with normal cellular metabolism. Consequently, a more holistic approach is needed when studying the PPP and designing experiments.

#### Future Perspectives

In the future, we aim to translate these *in vitro* findings into an animal CRC model to study the therapeutic properties of 6-AN and 5-FU drug combination treatment in mice. We are also generating and characterizing HCT116 CRC cells with *G6PD* gene knockout using the CRISPR/Cas9 system. We will examine the consequence of abrogating the main

enzyme of the PPP and test its effect on cancer cell growth and cell death. Future studies will also test the effect of knocking out *G6PD* in CRC *in vivo* models.

The monosaccharide mannose has recently been characterized as an inhibitor of cellular growth and impairs the oxidative phase of the PPP through inhibiting G6PD (DeRossi et al., 2006). Mannose is well-tolerated in humans and is negatively correlated with the metabolic enzyme phosphomannose isomerase (PMI) levels in the cells. Colorectal cancer cells are characterized by low levels of PMI and are, therefore, sensitive to mannose (Gonzalez et al., 2018), therefore, we will investigate the effect of mannose treatment in combination with 5-FU on CRC *in vitro* and *in vivo* models.

## REFERENCES

1. Abdel-Samad, R., Aouad, P., Gali-Muhtasib, H., Sweidan, Z., Hmadi, R., Kadara, H., . . . Darwiche, N. (2018). Mechanism of action of the atypical retinoid ST1926 in colorectal cancer: DNA damage and DNA polymerase  $\alpha$ . *American journal of cancer research*, 8(1), 39-55. Retrieved from <https://pubmed.ncbi.nlm.nih.gov/29416919>
2. <https://www.ncbi.nlm.nih.gov/pmc/articles/PMC5794720/>
3. Ahmed, D., Eide, P. W., Eilertsen, I. A., Danielsen, S. A., Eknæs, M., Hektoen, M., . . . Lothe, R. A. (2013). Epigenetic and genetic features of 24 colon cancer cell lines. *Oncogenesis*, 2(9), e71. doi:10.1038/oncsis.2013.35
4. Al Saleh, L. A., & Darwiche, N. (2018). *Pentose Phosphate Pathway in Colorectal Cancer Cells: Role of P53 and P21*. (Masters of Science). American University of Beirut, Saab Medical Library. (THES W 4 S163p 2018)
5. Almugadam, S. H., Trentini, A., Maritati, M., Contini, C., Rugna, G., Bellini, T., . . . Hanau, S. (2018). Influence of 6-aminonicotinamide (6AN) on Leishmania promastigotes evaluated by metabolomics: Beyond the pentose phosphate pathway. *Chem Biol Interact*, 294, 167-177. doi:10.1016/j.cbi.2018.08.014
6. American Cancer Society. (2020). Retrieved from <https://www.cancer.org/research/cancer-facts-statistics/all-cancer-facts-figures/cancer-facts-figures-2020.html>
7. Bader, D. A., & McGuire, S. E. (2020). Tumour metabolism and its unique properties in prostate adenocarcinoma. *Nat Rev Urol*, 17(4), 214-231. doi:10.1038/s41585-020-0288-x
8. Battaglin, F., Naseem, M., Lenz, H. J., & Salem, M. E. (2018). Microsatellite instability in colorectal cancer: overview of its clinical significance and novel perspectives. *Clin Adv Hematol Oncol*, 16(11), 735-745.
9. Belfi, C. A., Chatterjee, S., Gosky, D. M., Berger, S. J., & Berger, N. A. (1999). Increased sensitivity of human colon cancer cells to DNA cross-linking agents after GRP78 up-regulation. *Biochem Biophys Res Commun*, 257(2), 361-368. doi:10.1006/bbrc.1999.0472
10. Boyer, J., McLean, E. G., Aroori, S., Wilson, P., McCulla, A., Carey, P. D., . . . Johnston, P. G. (2004). Characterization of p53 wild-type and null isogenic colorectal cancer cell lines resistant to 5-fluorouracil, oxaliplatin, and irinotecan. *Clin Cancer Res*, 10(6), 2158-2167. doi:10.1158/1078-0432.ccr-03-0362
11. Brattain, M. G., Fine, W. D., Khaled, F. M., Thompson, J., & Brattain, D. E. (1981). Heterogeneity of malignant cells from a human colonic carcinoma. *Cancer Res*, 41(5), 1751-1756.
12. Budihardjo, II, Walker, D. L., Svingen, P. A., Buckwalter, C. A., Desnoyers, S., Eckdahl, S., . . . Kaufmann, S. H. (1998). 6-Aminonicotinamide sensitizes human tumor cell lines to cisplatin. *Clin Cancer Res*, 4(1), 117-130.
13. Cairns, R. A., Harris, I. S., & Mak, T. W. (2011). Regulation of cancer cell metabolism. *Nat Rev Cancer*, 11(2), 85-95. doi:10.1038/nrc2981

14. Carmona, A., & Freedland, R. A. (1990). Effect of 6-aminonicotinamide on pentose cycle activity in isolated hepatocytes. *Int J Biochem*, 22(6), 595-599. doi:10.1016/0020-711x(90)90034-z
15. Chou, T. C. (2010). Drug combination studies and their synergy quantification using the Chou-Talalay method. *Cancer Res*, 70(2), 440-446. doi:10.1158/0008-5472.Can-09-1947
16. Ciombor, K. K., Wu, C., & Goldberg, R. M. (2015). Recent therapeutic advances in the treatment of colorectal cancer. *Annu Rev Med*, 66, 83-95. doi:10.1146/annurev-med-051513-102539
17. Cremon, C., Stanghellini, V., Barbaro, M. R., Cogliandro, R. F., Bellacosa, L., Santos, J., . . . Barbara, G. (2017). Randomised clinical trial: the analgesic properties of dietary supplementation with palmitoylethanolamide and polydatin in irritable bowel syndrome. *Aliment Pharmacol Ther*, 45(7), 909-922. doi:10.1111/apt.13958
18. Dalvi, S. M., Patil, V. W., & Ramraje, N. N. (2012). The roles of glutathione, glutathione peroxidase, glutathione reductase and the carbonyl protein in pulmonary and extra pulmonary tuberculosis. *Journal of clinical and diagnostic research : JCDR*, 6(9), 1462-1465. doi:10.7860/JCDR/2012/4410.2533
19. De Angelis, P. M., Svendsrud, D. H., Kravik, K. L., & Stokke, T. (2006). Cellular response to 5-fluorouracil (5-FU) in 5-FU-resistant colon cancer cell lines during treatment and recovery. *Mol Cancer*, 5, 20. doi:10.1186/1476-4598-5-20
20. De Maria, S., Scognamiglio, I., Lombardi, A., Amodio, N., Caraglia, M., Carteni, M., . . . Stiuso, P. (2013). Polydatin, a natural precursor of resveratrol, induces cell cycle arrest and differentiation of human colorectal Caco-2 cell. *J Transl Med*, 11, 264. doi:10.1186/1479-5876-11-264
21. Dekker, E., Tanis, P. J., Vleugels, J. L. A., Kasi, P. M., & Wallace, M. B. (2019). Colorectal cancer. *Lancet*, 394(10207), 1467-1480. doi:10.1016/s0140-6736(19)32319-0
22. DeRossi, C., Bode, L., Eklund, E. A., Zhang, F., Davis, J. A., Westphal, V., . . . Freeze, H. H. (2006). Ablation of mouse phosphomannose isomerase (Mpi) causes mannose 6-phosphate accumulation, toxicity, and embryonic lethality. *J Biol Chem*, 281(9), 5916-5927. doi:10.1074/jbc.M511982200
23. Di Monaco, M., Pizzini, A., Gatto, V., Leonardi, L., Gallo, M., Brignardello, E., & Boccuzzi, G. (1997). Role of glucose-6-phosphate dehydrogenase inhibition in the antiproliferative effects of dehydroepiandrosterone on human breast cancer cells. *Br J Cancer*, 75(4), 589-592. doi:10.1038/bjc.1997.102
24. Dietrich, L. S., Friedland, I. M., & Kaplan, L. A. (1958). Pyridine nucleotide metabolism: mechanism of action of the niacin antagonist, 6-aminonicotinamide. *J Biol Chem*, 233(4), 964-968.
25. Dietrich, L. S., Muniz, O., Farinas, B., & Franklin, L. (1968). 6-aminonicotinamide-14C utilization by the 755 tumor and host liver tissue. *Cancer Res*, 28(8), 1652-1654.
26. Dore, M. P., Davoli, A., Longo, N., Marras, G., & Pes, G. M. (2016). Glucose-6-phosphate dehydrogenase deficiency and risk of colorectal cancer in Northern

- Sardinia: A retrospective observational study. *Medicine (Baltimore)*, 95(44), e5254. doi:10.1097/md.0000000000005254
27. Douillard, J. Y., Cunningham, D., Roth, A. D., Navarro, M., James, R. D., Karasek, P., . . . Rougier, P. (2000). Irinotecan combined with fluorouracil compared with fluorouracil alone as first-line treatment for metastatic colorectal cancer: a multicentre randomised trial. *Lancet*, 355(9209), 1041-1047. doi:10.1016/s0140-6736(00)02034-1
  28. Du, Q. H., Peng, C., & Zhang, H. (2013). Polydatin: a review of pharmacology and pharmacokinetics. *Pharm Biol*, 51(11), 1347-1354. doi:10.3109/13880209.2013.792849
  29. Duvel, K., Yecies, J. L., Menon, S., Raman, P., Lipovsky, A. I., Souza, A. L., . . . Manning, B. D. (2010). Activation of a metabolic gene regulatory network downstream of mTOR complex 1. *Mol Cell*, 39(2), 171-183. doi:10.1016/j.molcel.2010.06.022
  30. Eriksson, M., Ambroise, G., Ouchida, A. T., Lima Queiroz, A., Smith, D., Gimenez-Cassina, A., . . . Vakifahmetoglu-Norberg, H. (2017). Effect of Mutant p53 Proteins on Glycolysis and Mitochondrial Metabolism. *Molecular and cellular biology*, 37(24), e00328-00317. doi:10.1128/MCB.00328-17
  31. Fang, Z., Jiang, C., Feng, Y., Chen, R., Lin, X., Zhang, Z., . . . Jiang, W. (2016). Effects of G6PD activity inhibition on the viability, ROS generation and mechanical properties of cervical cancer cells. *Biochim Biophys Acta*, 1863(9), 2245-2254. doi:10.1016/j.bbamcr.2016.05.016
  32. Focaccetti, C., Bruno, A., Magnani, E., Bartolini, D., Principi, E., Dallaglio, K., . . . Albini, A. (2015). Effects of 5-fluorouracil on morphology, cell cycle, proliferation, apoptosis, autophagy and ROS production in endothelial cells and cardiomyocytes. *PLoS one*, 10(2), e0115686-e0115686. doi:10.1371/journal.pone.0115686
  33. Galluzzi, L., Kepp, O., Vander Heiden, M. G., & Kroemer, G. (2013). Metabolic targets for cancer therapy. *Nat Rev Drug Discov*, 12(11), 829-846. doi:10.1038/nrd4145
  34. Georgakilas, A. G., Martin, O. A., & Bonner, W. M. (2017). p21: A Two-Faced Genome Guardian. *Trends Mol Med*, 23(4), 310-319. doi:10.1016/j.molmed.2017.02.001
  35. Giacchetti, S., Perpoint, B., Zidani, R., Le Bail, N., Faggiuolo, R., Focan, C., . . . Levi, F. (2000). Phase III multicenter randomized trial of oxaliplatin added to chronomodulated fluorouracil-leucovorin as first-line treatment of metastatic colorectal cancer. *J Clin Oncol*, 18(1), 136-147. doi:10.1200/jco.2000.18.1.136
  36. Gonzalez, P. S., O'Prey, J., Cardaci, S., Barthelet, V. J. A., Sakamaki, J. I., Beaumatin, F., . . . Ryan, K. M. (2018). Mannose impairs tumour growth and enhances chemotherapy. *Nature*, 563(7733), 719-723. doi:10.1038/s41586-018-0729-3
  37. Gordon, G., Mackow, M. C., & Levy, H. R. (1995). On the mechanism of interaction of steroids with human glucose 6-phosphate dehydrogenase. *Arch Biochem Biophys*, 318(1), 25-29. doi:10.1006/abbi.1995.1199
  38. Hanahan, D., & Weinberg, R. A. (2011). Hallmarks of cancer: the next generation. *Cell*, 144(5), 646-674. doi:10.1016/j.cell.2011.02.013

39. Hanahan, D., & Weinberg, R. A. (2015). *Chapter 2: Hallmarks of Cancer: An organizing Principle for Cancer Medicine*.
40. Herken, H. (1968). Biosynthesis and action of dinucleotides containing 6-aminonicotinamide on membrane transport processes. *Arzneimittelforschung*, *18*(10), 1235-1245.
41. Hong, Y., Downey, T., Eu, K. W., Koh, P. K., & Cheah, P. Y. (2010). A 'metastasis-prone' signature for early-stage mismatch-repair proficient sporadic colorectal cancer patients and its implications for possible therapeutics. *Clin Exp Metastasis*, *27*(2), 83-90. doi:10.1007/s10585-010-9305-4
42. Huang, K., & Wu, L. D. (2018). Dehydroepiandrosterone: Molecular mechanisms and therapeutic implications in osteoarthritis. *J Steroid Biochem Mol Biol*, *183*, 27-38. doi:10.1016/j.jsbmb.2018.05.004
43. Jahani, M., Azadbakht, M., Norooznezhad, F., & Mansouri, K. (2017). l-arginine alters the effect of 5-fluorouracil on breast cancer cells in favor of apoptosis. *Biomed Pharmacother*, *88*, 114-123. doi:10.1016/j.biopha.2017.01.047
44. Jiang, P., Du, W., Wang, X., Mancuso, A., Gao, X., Wu, M., & Yang, X. (2011). p53 regulates biosynthesis through direct inactivation of glucose-6-phosphate dehydrogenase. *Nature cell biology*, *13*(3), 310-316. doi:10.1038/ncb2172
45. Jiang, P., Du, W., & Wu, M. (2014). Regulation of the pentose phosphate pathway in cancer. *Protein Cell*, *5*(8), 592-602. doi:10.1007/s13238-014-0082-8
46. Klinge, C. M., Clark, B. J., & Prough, R. A. (2018). Dehydroepiandrosterone Research: Past, Current, and Future. *Vitam Horm*, *108*, 1-28. doi:10.1016/bs.vh.2018.02.002
47. Kopetz, S. (2019). New therapies and insights into the changing landscape of colorectal cancer. *Nat Rev Gastroenterol Hepatol*, *16*(2), 79-80. doi:10.1038/s41575-018-0100-z
48. Koutcher, J. A., Alfieri, A. A., Stolfi, R. L., Devitt, M. L., Colofiore, J. R., Nord, L. D., & Martin, D. S. (1993). Potentiation of a three drug chemotherapy regimen by radiation. *Cancer Res*, *53*(15), 3518-3523.
49. Kowalik, M. A., Columbano, A., & Perra, A. (2017). Emerging Role of the Pentose Phosphate Pathway in Hepatocellular Carcinoma. *Front Oncol*, *7*, 87. doi:10.3389/fonc.2017.00087
50. Kruger, S., Ilmer, M., Kobold, S., Cadilha, B. L., Endres, S., Ormanns, S., . . . von Bergwelt-Baildon, M. (2019). Advances in cancer immunotherapy 2019 - latest trends. *J Exp Clin Cancer Res*, *38*(1), 268. doi:10.1186/s13046-019-1266-0
51. Langbein, S., Zerilli, M., Zur Hausen, A., Staiger, W., Rensch-Boschert, K., Lukan, N., . . . Coy, J. F. (2006). Expression of transketolase TKTL1 predicts colon and urothelial cancer patient survival: Warburg effect reinterpreted. *Br J Cancer*, *94*(4), 578-585. doi:10.1038/sj.bjc.6602962
52. Let's Talk Academy. (2018). Pentose Phosphate Pathway. Retrieved from <https://www.letstalkacademy.com/publication/read/pentose-phosphate-pathway>
53. Li, X.-L., Zhou, J., Chen, Z.-R., & Chng, W.-J. (2015). P53 mutations in colorectal cancer - molecular pathogenesis and pharmacological reactivation. *World journal of gastroenterology*, *21*(1), 84-93. doi:10.3748/wjg.v21.i1.84

54. Longley, D. B., Harkin, D. P., & Johnston, P. G. (2003). 5-fluorouracil: mechanisms of action and clinical strategies. *Nat Rev Cancer*, 3(5), 330-338. doi:10.1038/nrc1074
55. Mader, R. M., Muller, M., & Steger, G. G. (1998). Resistance to 5-fluorouracil. *Gen Pharmacol*, 31(5), 661-666. doi:10.1016/s0306-3623(98)00191-8
56. Malumbres, M., & Barbacid, M. (2009). Cell cycle, CDKs and cancer: a changing paradigm. *Nature Reviews Cancer*, 9(3), 153-166. doi:10.1038/nrc2602
57. Marmol, I., Sanchez-de-Diego, C., Pradilla Dieste, A., Cerrada, E., & Rodriguez Yoldi, M. J. (2017). Colorectal Carcinoma: A General Overview and Future Perspectives in Colorectal Cancer. *Int J Mol Sci*, 18(1). doi:10.3390/ijms18010197
58. Martinez-Outschoorn, U. E., Peiris-Pages, M., Pestell, R. G., Sotgia, F., & Lisanti, M. P. (2017). Cancer metabolism: a therapeutic perspective. *Nat Rev Clin Oncol*, 14(1), 11-31. doi:10.1038/nrclinonc.2016.60
59. McConnell, D. D., McGreevy, J. W., Williams, M. N., & Litofsky, N. S. (2018). Do Anti-Oxidants Vitamin D(3,) Melatonin, and Alpha-Lipoic Acid Have Synergistic Effects with Temozolomide on Cultured Glioblastoma Cells? *Medicines (Basel)*, 5(2). doi:10.3390/medicines5020058
60. Mele, L., la Noce, M., Paino, F., Regad, T., Wagner, S., Liccardo, D., . . . Papaccio, F. (2019). Glucose-6-phosphate dehydrogenase blockade potentiates tyrosine kinase inhibitor effect on breast cancer cells through autophagy perturbation. *J Exp Clin Cancer Res*, 38(1), 160. doi:10.1186/s13046-019-1164-5
61. Mele, L., Paino, F., Papaccio, F., Regad, T., Boocock, D., Stiuso, P., . . . Desiderio, V. (2018). A new inhibitor of glucose-6-phosphate dehydrogenase blocks pentose phosphate pathway and suppresses malignant proliferation and metastasis in vivo. *Cell Death Dis*, 9(5), 572. doi:10.1038/s41419-018-0635-5
62. Micali, G., Lacarrubba, F., Nasca, M. R., & Schwartz, R. A. (2014). Topical pharmacotherapy for skin cancer: part I. Pharmacology. *J Am Acad Dermatol*, 70(6), 965.e961-912; quiz 977-968. doi:10.1016/j.jaad.2013.12.045
63. Montalban-Arques, A., & Scharl, M. (2019). Intestinal microbiota and colorectal carcinoma: Implications for pathogenesis, diagnosis, and therapy. *EBioMedicine*, 48, 648-655. doi:10.1016/j.ebiom.2019.09.050
64. Nee, J., Chippendale, R. Z., & Feuerstein, J. D. (2020). Screening for Colon Cancer in Older Adults: Risks, Benefits, and When to Stop. *Mayo Clin Proc*, 95(1), 184-196. doi:10.1016/j.mayocp.2019.02.021
65. Nguyen, H. T., & Duong, H. Q. (2018). The molecular characteristics of colorectal cancer: Implications for diagnosis and therapy. *Oncol Lett*, 16(1), 9-18. doi:10.3892/ol.2018.8679
66. Oines, M., Helsingen, L. M., Bretthauer, M., & Emilsson, L. (2017). Epidemiology and risk factors of colorectal polyps. *Best Pract Res Clin Gastroenterol*, 31(4), 419-424. doi:10.1016/j.bpg.2017.06.004
67. Oncomine. Retrieved from <https://www.oncomine.org/resource/login.html>
68. Pai, E. F., & Schulz, G. E. (1983). The catalytic mechanism of glutathione reductase as derived from x-ray diffraction analyses of reaction intermediates. *J Biol Chem*, 258(3), 1752-1757.

69. Patra, K. C., & Hay, N. (2014). The pentose phosphate pathway and cancer. *Trends Biochem Sci*, 39(8), 347-354. doi:10.1016/j.tibs.2014.06.005
70. Pavlova, N. N., & Thompson, C. B. (2016). The Emerging Hallmarks of Cancer Metabolism. *Cell Metab*, 23(1), 27-47. doi:10.1016/j.cmet.2015.12.006
71. Penkowa, M., Quintana, A., Carrasco, J., Giralt, M., Molinero, A., & Hidalgo, J. (2004). Metallothionein prevents neurodegeneration and central nervous system cell death after treatment with gliotoxin 6-aminonicotinamide. *J Neurosci Res*, 77(1), 35-53. doi:10.1002/jnr.20154
72. Polimeni, M., Voena, C., Kopecka, J., Riganti, C., Pescarmona, G., Bosia, A., & Ghigo, D. (2011). Modulation of doxorubicin resistance by the glucose-6-phosphate dehydrogenase activity. *Biochem J*, 439(1), 141-149. doi:10.1042/bj20102016
73. Punt, C. J., Koopman, M., & Vermeulen, L. (2017). From tumour heterogeneity to advances in precision treatment of colorectal cancer. *Nat Rev Clin Oncol*, 14(4), 235-246. doi:10.1038/nrclinonc.2016.171
74. Rajesh, E., Sankari, L. S., Malathi, L., & Krupaa, J. R. (2015). Naturally occurring products in cancer therapy. *Journal of pharmacy & bioallied sciences*, 7(Suppl 1), S181-S183. doi:10.4103/0975-7406.155895
75. Rajput, A., Dominguez San Martin, I., Rose, R., Beko, A., Levea, C., Sharratt, E., . . . Wang, J. (2008). Characterization of HCT116 human colon cancer cells in an orthotopic model. *J Surg Res*, 147(2), 276-281. doi:10.1016/j.jss.2007.04.021
76. Ren, F., Yang, X., Hu, Z. W., Wong, V. K. W., Xu, H. Y., Ren, J. H., . . . Chen, J. (2019). Niacin analogue, 6-Aminonicotinamide, a novel inhibitor of hepatitis B virus replication and HBsAg production. *EBioMedicine*, 49, 232-246. doi:10.1016/j.ebiom.2019.10.022
77. Rudd, D. (2012). Elsevier's integrated review biochemistry 2nd edition [Book Review]. *Australian Journal of Medical Science*, 33(4), 182.
78. Sabates-Bellver, J., Van der Flier, L. G., de Palo, M., Cattaneo, E., Maake, C., Rehrauer, H., . . . Marra, G. (2007). Transcriptome profile of human colorectal adenomas. *Mol Cancer Res*, 5(12), 1263-1275. doi:10.1158/1541-7786.Mcr-07-0267
79. Salakou, S., Kardamakis, D., Tsamandas, A. C., Zolota, V., Apostolakis, E., Tzelepi, V., . . . Dougenis, D. (2007). Increased Bax/Bcl-2 ratio up-regulates caspase-3 and increases apoptosis in the thymus of patients with myasthenia gravis. *In Vivo*, 21(1), 123-132.
80. Sánchez-Gundín, J., Fernández-Carballido, A. M., Martínez-Valdivieso, L., Barreda-Hernández, D., & Torres-Suárez, A. I. (2018). New Trends in the Therapeutic Approach to Metastatic Colorectal Cancer. *Int J Med Sci*, 15(7), 659-665. doi:10.7150/ijms.24453
81. Sara, J. D., Kaur, J., Khodadadi, R., Rehman, M., Lobo, R., Chakrabarti, S., . . . Grothey, A. (2018). 5-fluorouracil and cardiotoxicity: a review. *Ther Adv Med Oncol*, 10, 1758835918780140. doi:10.1177/1758835918780140
82. Schwaederle, M., Chattopadhyay, R., Kato, S., Fanta, P. T., Banks, K. C., Choi, I. S., . . . Kurzrock, R. (2017). Genomic alterations in circulating tumor DNA from diverse cancer patients identified by next-generation sequencing. *Cancer Research*, canres.0885.2017. doi:10.1158/0008-5472.CAN-17-0885



83. Shamseddine, A., Saleh, A., Charafeddine, M., Seoud, M., Mukherji, D., Temraz, S., & Sibai, A. M. (2014). Cancer trends in Lebanon: a review of incidence rates for the period of 2003–2008 and projections until 2018. *Population Health Metrics*, *12*(1), 4. doi:10.1186/1478-7954-12-4
84. Shibuya, N., Inoue, K., Tanaka, G., Akimoto, K., & Kubota, K. (2015). Augmented pentose phosphate pathway plays critical roles in colorectal carcinomas. *Oncology*, *88*(5), 309-319. doi:10.1159/000369905
85. Shimizu, T., Inoue, K., Hachiya, H., Shibuya, N., Shimoda, M., & Kubota, K. (2014). Frequent alteration of the protein synthesis of enzymes for glucose metabolism in hepatocellular carcinomas. *J Gastroenterol*, *49*(9), 1324-1332. doi:10.1007/s00535-013-0895-x
86. Siegel, R. L., Miller, K. D., & Jemal, A. (2020). Cancer statistics, 2020. *CA Cancer J Clin*, *70*(1), 7-30. doi:10.3322/caac.21590
87. Sims, J. L., Sikorski, G. W., Catino, D. M., Berger, S. J., & Berger, N. A. (1982). Poly(adenosinediphosphoribose) polymerase inhibitors stimulate unscheduled deoxyribonucleic acid synthesis in normal human lymphocytes. *Biochemistry*, *21*(8), 1813-1821. doi:10.1021/bi00537a017
88. Skrzypczak, M., Goryca, K., Rubel, T., Paziewska, A., Mikula, M., Jarosz, D., . . . Ostrowski, J. (2010). Modeling oncogenic signaling in colon tumors by multidirectional analyses of microarray data directed for maximization of analytical reliability. *PLoS One*, *5*(10). doi:10.1371/journal.pone.0013091
89. Stolfi, R. L., Colofiore, J. R., Nord, L. D., Koutcher, J. A., & Martin, D. S. (1992). Biochemical modulation of tumor cell energy: regression of advanced spontaneous murine breast tumors with a 5-fluorouracil-containing drug combination. *Cancer Res*, *52*(15), 4074-4081.
90. Sukhatme, V. P., & Chan, B. (2012). Glycolytic cancer cells lacking 6-phosphogluconate dehydrogenase metabolize glucose to induce senescence. *FEBS Lett*, *586*(16), 2389-2395. doi:10.1016/j.febslet.2012.05.052
91. TCGA. (2011). The Cancer Genome Atlas - Colon and Rectum Adenocarcinoma Gene Expression Data. Retrieved from <http://tcga-data.nci.nih.gov/tcga/>
92. Torres, N. P., Lee, A. Y., Giaever, G., Nislow, C., & Brown, G. W. (2013). A high-throughput yeast assay identifies synergistic drug combinations. *Assay Drug Dev Technol*, *11*(5), 299-307. doi:10.1089/adt.2012.503
93. Tsouko, E., Khan, A. S., White, M. A., Han, J. J., Shi, Y., Merchant, F. A., . . . Frigo, D. E. (2014). Regulation of the pentose phosphate pathway by an androgen receptor-mTOR-mediated mechanism and its role in prostate cancer cell growth. *Oncogenesis*, *3*(5), e103. doi:10.1038/oncsis.2014.18
94. Varnes, M. E. (1988). Inhibition of pentose cycle of A549 cells by 6-aminonicotinamide: consequences for aerobic and hypoxic radiation response and for radiosensitizer action. *NCI Monogr*(6), 199-203.
95. Vassallo, S. U. (2019). Athletic Performance Enhancers. In L. S. Nelson, M. A. Howland, N. A. Lewin, S. W. Smith, L. R. Goldfrank, & R. S. Hoffman (Eds.), *Goldfrank's Toxicologic Emergencies, 11e*. New York, NY: McGraw-Hill Education.

96. Vogelstein, B., Papadopoulos, N., Velculescu, V. E., Zhou, S., Diaz, L. A., Jr., & Kinzler, K. W. (2013). Cancer genome landscapes. *Science*, *339*(6127), 1546-1558. doi:10.1126/science.1235122
97. Waldman, T., Kinzler, K. W., & Vogelstein, B. (1995). p21 is necessary for the p53-mediated G1 arrest in human cancer cells. *Cancer Res*, *55*(22), 5187-5190.
98. World Cancer Research Fund. (2018). Retrieved from <https://www.wcrf.org/dietandcancer>
99. World Health Organization. (2018). Retrieved from <https://www.who.int/en/news-room/fact-sheets/detail/cancer>
100. Xie, Y.-H., Chen, Y.-X., & Fang, J.-Y. (2020). Comprehensive review of targeted therapy for colorectal cancer. *Signal Transduction and Targeted Therapy*, *5*(1), 22. doi:10.1038/s41392-020-0116-z
101. Ying, H., Kimmelman, A. C., Lyssiotis, C. A., Hua, S., Chu, G. C., Fletcher-Sanankone, E., . . . DePinho, R. A. (2012). Oncogenic Kras maintains pancreatic tumors through regulation of anabolic glucose metabolism. *Cell*, *149*(3), 656-670. doi:10.1016/j.cell.2012.01.058
102. Zackheim, H. S. (1975). Treatment of psoriasis with 6-aminonicotinamide. *Arch Dermatol*, *111*(7), 880-882.
103. Zhang, N., Yin, Y., Xu, S.-J., & Chen, W.-S. (2008). 5-Fluorouracil: mechanisms of resistance and reversal strategies. *Molecules (Basel, Switzerland)*, *13*(8), 1551-1569. doi:10.3390/molecules13081551
104. Zhang, X., Zhang, X., Li, Y., Shao, Y., Xiao, J., Zhu, G., & Li, F. (2017). PAK4 regulates G6PD activity by p53 degradation involving colon cancer cell growth. *Cell Death Dis*, *8*(5), e2820. doi:10.1038/cddis.2017.85
105. Zumoff, B., Levin, J., Rosenfeld, R. S., Markham, M., Strain, G. W., & Fukushima, D. K. (1981). Abnormal 24-hr mean plasma concentrations of dehydroisoandrosterone and dehydroisoandrosterone sulfate in women with primary operable breast cancer. *Cancer Res*, *41*(9 Pt 1), 3360-3363.